

Review

Non-Thermal Plasma Coupled with Catalyst for the Degradation of Water Pollutants: A Review

Mariaconcetta Russo, Giuseppina Iervolino *, Vincenzo Vaiano  and Vincenzo Palma 

Department of Industrial Engineering, University of Salerno, via Giovanni Paolo II, 132, 84084 Fisciano, Italy; marrusso@unisa.it (M.R.); vvaiano@unisa.it (V.V.); vpalma@unisa.it (V.P.)

* Correspondence: giervolino@unisa.it; Tel.: +39-089-964-006

Received: 11 November 2020; Accepted: 7 December 2020; Published: 9 December 2020



Abstract: Non-thermal plasma is one of the most promising technologies used for the degradation of hazardous pollutants in wastewater. Recent studies evidenced that various operating parameters influence the yield of the Non-Thermal Plasma (NTP)-based processes. In particular, the presence of a catalyst, suitably placed in the NTP reactor, induces a significant increase in process performance with respect to NTP alone. For this purpose, several researchers have studied the ability of NTP coupled to catalysts for the removal of different kind of pollutants in aqueous solution. It is clear that it is still complicated to define an optimal condition that can be suitable for all types of contaminants as well as for the various types of catalysts used in this context. However, it was highlighted that the operational parameters play a fundamental role. However, it is often difficult to understand the effect that plasma can induce on the catalyst and on the production of the oxidizing species most responsible for the degradation of contaminants. For this reason, the aim of this review is to summarize catalytic formulations coupled with non-thermal plasma technology for water pollutants removal. In particular, the reactor configuration to be adopted when NTP was coupled with a catalyst was presented, as well as the position of the catalyst in the reactor and the role of the main oxidizing species. Furthermore, in this review, a comparison in terms of degradation and mineralization efficiency was made for the different cases studied.

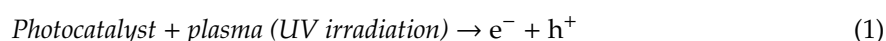
Keywords: non-thermal plasma coupled catalyst; water pollution; operating condition; DBD

1. Introduction

Non-thermal plasma technologies (NTP) have been proved to be an emerging alternative for water pollutants treatment [1,2]. The degradation of hazardous pollutants from water is one of the most critical issues regarding environmental pollution [3,4]. Wastewater treatment is generally based on physical and biological processes. However, these kinds of treatments are often inefficient to remove pollutants like pesticides, dyes, and pharmaceutical compounds, which are increasingly present in wastewater [5–7]. For this reason, advanced oxidation processes (AOPs) have been considered possible alternatives thanks to their extreme oxidizing capacity and their efficiency in the removal of bio-recalcitrant compounds. Among these, non-thermal plasma represents an innovative AOP for water treatment [1]. With respect to “thermal” plasma, the NTP system maintains at relatively low temperatures [8] and is able to generate charge carriers [9–11].

The most used method to create NTP is gas discharge in which the energy from the electric field is accumulated by the electrons through collision, and only a fraction of the energy will then be transferred to other molecules [12]. There are several methods for NTP generation such as dielectric barrier discharge (DBD), gliding arc discharge (GAD), corona discharge, radio frequency (RF) plasma, microwave discharge (MD), and jet plasma [13]. As reported in the literature, NTP technology is widely used for different applications [14] and especially for the degradation of pollutants from

wastewater [15–17]. It is well known that the NTP process could produce active species such as O_3 , H_2O_2 , $\bullet OH$, $\bullet O$, which play a key role in the oxidative degradation of pollutants. However, some disadvantages of NTP “alone” in the degradation of organic contaminants is mainly linked to the formation of unwanted by-products that can limit its industrial applications [18]. To overcome these limitations, an interesting strategy, consisting of the combination of NTP and heterogeneous catalysis, has been proposed to enhance pollutant degradation efficiency and, simultaneously, reduce the formation of reaction by-products [19–21]. The effect of NTP combined with catalysts enhances the generation of different types of active species (such as hydroxyls) and the activity and stability of photocatalytic materials [22–26]. For example, when a photocatalyst is introduced into an NTP reactor, the generation of the active species through the plasma, including ultraviolet light, can induce photocatalytic reactions, for example through the following path [27]:



In this way, the catalyst not only reduces the activation energy of the oxidation reactions but also regulates the selectivity towards the desired products.

How can catalyst and non-thermal plasma be combined? There are two ways [28]:

- Single-stage system or in-plasma catalysis (IPC) system: the catalyst is introduced to the discharge zone, inducing heterogeneous reactions in the system due to the interaction of catalyst and plasma.
- Plasma post-processing or plasma pre-processing (PPC): the catalyst is introduced upstream or downstream of the discharge region.

The IPC configuration allows the catalyst to influence the chemical nature of the process by interacting directly with the plasma and with the reaction products. On the other hand, in the case of the PPC configuration, the longer-lived excited species and the products obtained from the plasma reaction with the solution to be treated can interact with the catalyst located downstream (or upstream) of the plasma itself [29]. Generally, the incorporation of the catalyst can occur in the plasma in various forms as foam [30], honeycomb monolith [31], coating on the reactor walls or electrodes, or a packed bed [32].

The aim of this review is to provide a wide-ranging overview on the synergistic effect of NTP with catalysts to achieve the degradation of pollutants from water and wastewater and to offer the reader useful tools and information to understand this kind of application in wastewater treatment in order to define the most suitable choice for the case study examined.

2. Reactor Configurations

Non-thermal plasma reactors can be divided into different categories with respect to: the type of power supply (DC, pulse, DC and pulse, AC, AC and DC, RF), presence of a dielectric barrier or catalyst, geometry, mode of discharge, polarity, and voltage level and gas composition. In this section, the conventional NTP reactor widely used in many applications are described: dielectric barrier discharge (DBD), gliding arc discharge (GAD), corona discharge, and surface plasma discharge.

2.1. Dielectric Barrier Discharge Reactor

DBD (Figure 1a), also known as “ozone production discharge”, is generally a discharge between two electrodes separated by insulating dielectric barriers generating one or more insulating layers in the current path between metal electrodes [33]. In a DBD, the average temperature of high-energy electrons is very high, over the range of 10,000–100,000 K, but the actual gas temperature is close to the environment temperature. By electron impact ionization and excitation, source gases can produce

active radicals, ions, excited atoms, and molecular species [34]. This kind of reactor configuration is characterized by different advantages, such as the possibility to work at atmospheric pressure, the presence of a homogeneous, large-volume and stable plasma area; be a flexible configuration for a possible scale up; the possibility of easily coupling this reactor configuration to a catalyst [35].

2.2. Gliding Arc Discharge

Gliding arc discharge (GAD), also considered as a “transitional plasma”, is generated by applying an electrical field across two or more electrodes in a laminar or turbulent gas flow [36]. Generally, a gliding arc system offers the opportunity to work efficiently with a wide flow rate range and with high power levels (up to several kV). Moreover, unlike other plasma systems, GAD is characterized by an electron density (10^{23} – 10^{24} m⁻³) close to that of a thermal plasma [37]. A typical scheme of gliding arc discharge is shown in Figure 1b [38]. In addition, in this case, GAD configuration is characterized by different advantages, such as the possibility of working at atmospheric pressure and simple configuration that requires low investment costs. Furthermore, this type of configuration guarantees plasma with a high electron density and powerful transient plasma [35].

2.3. Corona Discharge

The corona discharge can be defined as an electrical discharge caused by the ionization of a gas (for example air) between two electrodes powered by high voltage. In many applications, corona discharge is generated by using a pin to plate surface configuration (Figure 1c) [39] and it is possible to define corona as an inhomogeneous discharge [35]. Corona discharge is an interesting technology for the treatment of various pollutants even if it has several problems that limit further application, such as a high cost for the pulsed power supply, a high malfunction rate, and short life of the electrodes [40].

2.4. Surface Plasma Discharge

A typical scheme of surface plasma discharge is shown in Figure 1d. It is characterized by one of the electrodes that cover one side of the dielectric barrier completely while the other electrode only partially covers it. The plasma is generated next to this dielectric surface, which is in contact with the gas [41]. Once the electric field is applied, the surface plasma covers the entire dielectric surface [42]. The charge after a few nanoseconds begins to accumulate on the dielectric surface, which could reduce the electric fields outside the dielectric, extinguishing the discharge. Other kinds of configuration include radiofrequency (RF) plasma in which plasma is generated in a gas flow via an externally induced RF field. This gas is filed in an oscillating electromagnetic field and plasma is formed by different electrodes placed outside the reactor. Another one is microwave plasma or microwave reactor where plasma is generated using a magnetron that delivers the microwave. After the radiation is absorbed, heat and gas are produced in the process, initiating ionization reactions by inelastic collisions [43].

2.5. Catalytic Non-Thermal Plasma: Reactor Configuration

The NTP combined with the catalyst configurations have attracted a lot of attention in recent years since. As mentioned above, the use of a catalyst in an NTP reactor allows to promote the efficiency of this system through the thrust production of highly oxidizing species. However, it is important to understand how the catalyst must be introduced into the NTP reactor in order to improve its performance. It is also important to identify the best catalyst “formulation”, one that is not only chemical, but also structural: the catalyst can be in powder form, but it can also have macroscopic characteristics, for example pellets, spheres, and sheets. Therefore, it is essential to identify how the catalyst can be housed in the NTP reactor, but this aspect also depends on the reactor configuration (whether it is a DBD, PDP, or a GDC).

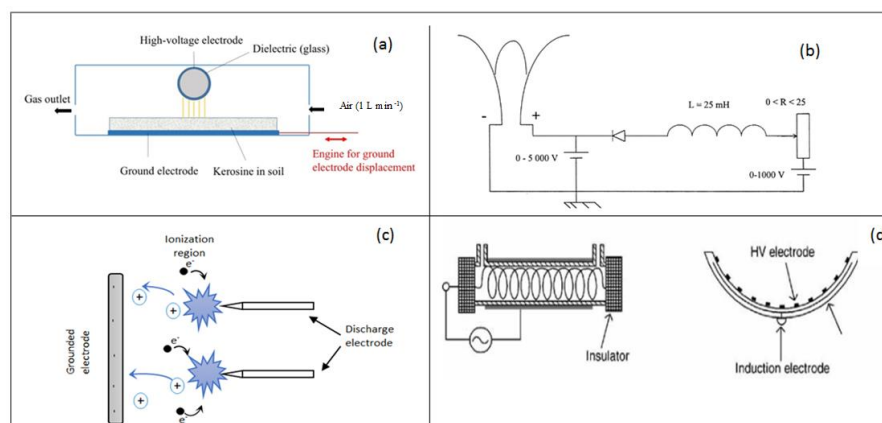


Figure 1. Typical scheme of the main plasma reactor configuration: (a) Dielectric barrier discharge [35], (b) Gliding arc gas discharge [38], (c) corona discharge [44], (d) surface discharge reactor [45].

For example, a dielectric packed bed reactor has attracted more attention for its environmental applications. Unlike an empty DBD reactor, the packing beads improve the electric field near the contact points, from which is generated higher electron energies, causing more electron impact collisions and consequently a greater production of reactive species [46]. The pellets exposed to an external electric field determine a spontaneous polarization in the direction of the electric field, resulting in a high electric field at the contact points of the pellets [45]. Furthermore, the use of pellets allows for a more uniform distribution of gas flow and discharge in the reactor, even if it is disadvantageous in terms of pressure drop [47]. This kind of system is one of the most popular reactor configurations used for plasma-catalysis where the plasma discharge is introduced right on the catalyst surface, which enhances the properties of the catalyst and its corresponding performance.

It has been reported that metal catalysts not only adsorb the pollutants but could also transform O_3 and H_2O_2 into $\bullet OH$ radicals, the main reactive species for pollutant degradation [48].

Some papers on the use of DBD reactor coupled with a catalyst are mentioned below:

- In the first study [49], the catalyst employed is Ag_3PO_4 on ACFs (activated carbon fibers) used as support previously cut into rectangle. The catalyst was wrapped around the inner wall of the inner cylinder of the reactor on which the solution, recirculated by a peristaltic pump, descends, creating a uniform liquid wall, thus promoting an intimate contact between plasma and the pollutant.
- Nguyen et al. reported the use of the same reactor configuration coupled with Ag/Al_2O_3 for the removal of NO_x emissions. The catalyst was placed inside the discharge zone, using two porous ceramic rings to assist in fixing the catalyst position in the reactor where the process gas was also present [50].
- Shayan Hoseini et al. reported the removal of volatile organic compounds, BTX (benzene, toluene and xylene), using manganese oxide nano-catalysts synthesized starting from spent batteries. In this case, the catalyst was shaped in the form of 1 mm pellets and subsequently placed into the reactor. Both IPC (in plasma catalysis) and PPC (post plasma catalysis) tests were conducted. The difference between the two configurations is that, in the IPC configuration, the catalyst was placed in the plasma region while, in the PPC configuration, the catalyst was placed after the plasma region. The results show that there is no significant difference between these two types of catalyst location in the plasma reactor and one of these configurations can be selected according to other operating conditions such as the type of plasma reactor or the nature of the catalysts [51].
- Iervolino et al. reported the use of DBD coupled with Fe_2O_3 immobilized on glass spheres for Acid Orange 7 degradation. The experimental tests were conducted in a falling film DBD reactor

- with a cylindrical configuration and at a tilt angle of 30°. The catalytic packed material was introduced in the discharge zone and on its surface the solution to be treated flows like a film [18].
- Bi₂WO₆-rMoS₂ nanocomposite was used in the dielectric barrier discharge (DBD) reactor for the sulfamethoxazole degradation in aqueous solution. In this case, the catalyst was in powder form and it was put on the inner of the circular quartz reactor, also in this case at the discharge area [52].
 - DBD plasma combined with TiO₂/ACFs was used for the triclocarban degradation. In this case, the catalyst was inserted inside the quartz reactor in correspondence with the discharge area, in contact with the solution to be treated, which flowed on the catalyst itself [53].
 - DBD plasma and ACFs were used for the degradation of triclosan in aqueous solution. In this case, the catalyst (ACFs) was positioned exactly in the discharge area and the solution to be treated was recirculated onto it, creating a liquid film, whose thickness was kept at about 1 mm [54].

The DBD configuration is among the most used reactor configurations in plasma-catalyst technology for pollutant degradation; however, other kinds of reactor configurations coupled with catalyst are reported in the literature.

In particular, as regard the hexachlorobenzene (H₆CB₂) removal for gas phase, the use of gliding arc (GA) plasma combined with V₂O₅-WO₃-TiO₂ catalyst has been reported. The reactor configuration includes rotating GA plasma developed inside a reactor, a downstream catalyst, and a high voltage power supply. In this case, the catalyst was located behind the plasma region, i.e., in the post-plasma region [55]. Min-Hao Yuan et al. studied the degradation of Vinyl Chloride with Pt/Al₂O₃ using atmospheric-pressure radio frequency discharge. The atmospheric-pressure plasma jet reactor consists of the following three subsystems:

- (1) feed gas;
- (2) plasma jet;
- (3) effluent gas analysis.

The catalyst composed of 0.23-wt% Pt supported on γ -Al₂O₃ was introduced at the end of the inner electrode. The distance between it and the top of the catalyst bed is 2 cm [56].

Kirkpatrick et al. reported the combination of pulsed positive streamer corona discharge with a platinum–rhodium catalyst for removal of toluene, acetonitrile, and nitrogen oxides. In the present study, a corona discharge reactor was employed, constructed of glass where the plasma discharge occurs between two reticulated vitreous carbon (RVC) disks. The downstream disk is coated with platinum and rhodium catalysts supported on RVC, a material that may be used as an electrode material in pulsed corona discharge reactors. The catalyst disk is characterized by 100 pores per inch RVC facing the discharge region; a substrate was first used to apply a graphitic layer to increase surface area. Subsequently platinum and rhodium were added to the graphitic coat [57]. In the last reported study [58], the plasma-catalytic degradation of benzene over Ag–Ce bimetallic oxide catalysts using hybrid surface/packed-bed discharge plasma is analysed. In particular, the present work analyses four plasma-catalysis systems, as schematized in Figure 2:

- Systems A and C are termed IPC systems, where the catalysts are packed inside region I (surface discharge region) and region II (packed-bed discharge region), respectively.
- Systems B and D, where the catalyst was placed downstream region I and region II to compose the PPC systems, respectively.

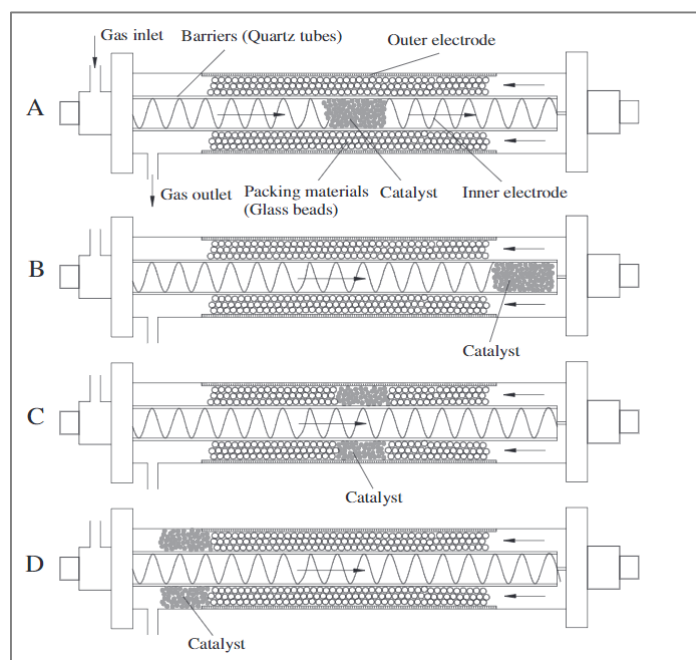


Figure 2. Different plasma-catalysis systems in IPC and PPC configurations: (A) catalysts were placed in the region I, (B) catalysts were placed downstream the region I, (C) catalysts were placed in the region II, (D) catalysts were placed downstream the region II [58].

The two different configurations determine distinct effects because in the IPC configuration, plasma-catalysis process may facilitate the electron and photon induced processes, change the discharge characteristic, and generate active species responsible for the degradation reaction, while in the PPC configuration, only long-lived species (such as O_3) and some stable organic intermediates generated by discharge plasma would be involved in plasma-catalytic surface reactions. From the results, they demonstrate that the PPC process is more efficient than the IPC reaction. This effect could be attributed to their efficiency to catalytically decompose ozone. Furthermore, the best result in terms of benzene degradation was obtained with catalysts packed downstream the region II (system D). It is interesting to note that, as reported by the authors, packing the catalyst support ($\gamma-Al_2O_3$) into region II, has little impact on benzene degradation efficiency [58].

2.6. Physical–Chemical Effects of Plasma Coupled with Catalyst

When the non-thermal plasma is coupled with a catalyst, the plasma can influence the characteristics of the catalytic material and vice versa, according to different aspects:

- The dispersion of active catalytic components could be enhanced by the discharge of NTP [59].
- The oxidation state of the material can be influenced by plasma discharge [60].
- Enhancement of a specific surface area due to plasma discharge [46].
- The dielectric constant of catalytic material can generate more microdischarges and create a strong electric field at the corners and edges [61].

According to results published in the literature, the oxidation state of the material can be influenced when exposed to plasma discharge [60]. In this paper, the authors reported the decomposition of acetaldehyde combining with gold-based catalysts. From XPS results, they notify that for the fresh catalyst pure element Au peaks are at 83.9 and 87.5 eV, respectively, while after plasma treatment, two new peaks appeared corresponding to AuO_x at 84.80 and 88.50 eV. The same considerations about the influence of discharge on oxidation state are reported also in other works [62,63]. To support the results obtained in terms of the catalytic specific surface area improvement by NTP, Kai Li et al. reported in their study the effects of NTP on the specific surface area of Fe/MCSAC (microwave coconut

shell activated carbon catalysts) used in a DBD plasma reactor for low-temperature catalytic hydrolysis of CS₂ [27]. In fact, from the experimental results, it was possible to observe an improved Fe particle dispersion due to NTP, an increasing of specific surface area, and a decrease in Fe particle size. Thus, the NTP can lead to a more uniform dispersion of supported species, smaller particle size, and higher specific surface area. This showed better catalytic activity. Specifically, the results showed that Fe/MCSAC catalysts with NTP modification presents better performance in terms of hydrolysed CS₂, using as the optimal reactor configuration coaxial cylinders, a modified atmosphere containing NH₃ and a treatment time equal to 10 min at 6.8 kV [64]. Furthermore, by focusing attention on the synergistic effect of the catalyst with NTP, the presence of heterogeneous catalysts may increase the production of active species, influencing the degradation mechanism of contaminants. For example, Tarkwa et al. reported that the presence of a heterogeneous catalyst in a gliding arc plasma reactor enhances the generation of reactive species, i.e., •OH and consequently the degradation of target pollutant, Orange G, from aqueous solution [65]. The same consideration has been made by other studies. For example, by combining plasma with the catalyst, it is possible to increase the adsorption capacity of species possessing high oxidation ability. In the literature, it is reported that the catalyst (for example, active carbon fibers with TiO₂) is able to adsorb O₃ produced by the DBD plasma favouring the production of •OH radicals [53]. Furthermore, in the presence of TiO₂, it is possible to exploit the UV irradiation produced by the plasma ($\lambda < 385$ nm) in order to generate a highly reactive hole–electron pair, capable of leading to the formation of other oxidizing species. Reddy et al. reported that the presence of a catalyst in the NTP reactors improves phenol degradation, because it is able to both enhance the life time of short-lived oxidized species produced by NTP and facilitate the formation of secondary oxidants, such as the atomic oxygen through the O₃ decomposition [66]. This confirms that the DBD-assisted catalytic process offers the possibility to obtain more reactive species able to react with different pollutants, preventing by-product formation.

3. Application of Catalytic-Assisted NTP for Water Treatment

3.1. Decontamination of Pharmaceutical Compounds

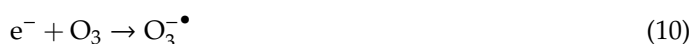
In the last years, the abuse of drugs has increased the diversity of pollutants into the environment. Because of their low biodegradability and high chemical stability, different pharmaceutical compounds do not get completely degraded during wastewater treatment processes. The combined effect of NTP with a catalyst is reported as a promising technology for the removal of pharmaceutical contaminants from wastewater. Shi Gong et al. reported the degradation of Levofloxacin (LFX) by non-thermal plasma (DBD) combined with Ag₃PO₄/activated carbon fibers [49]. They reported that the degradation efficiency of LFX increases with the increase of discharge voltage, liquid circulation velocity, catalyst dosage and, moreover, low value of pH favours LFX degradation. In particular, the results showed that, with the increase of Ag₃PO₄/ACFs catalysts dosage, an increase in LFX degradation was observed. In fact, with a higher catalyst dosage, the reaction area is wider; therefore, a greater amount of active species is irradiated by the light emitted from the plasma, and a greater number of reactive species which contribute to improving the degradation efficiency of the LFX is produced [49]. Moreover, Ag₃PO₄/ACFs catalysts also show good recycling ability and significantly increase the mineralization efficiency of LFX. Specific experiments were carried out in the presence of different radical scavengers. The results demonstrate that the OH radicals play the most important role in the degradation of LFX, followed by h⁺ and H radicals. However, if the production of O₃ is considered, in this case, it is reported that the addition of the Ag₃PO₄/ACFs catalyst led to a decrease in the concentration of O₃ produced, compared to that observed with NTP in the absence of catalyst. Probably, the reason for O₃ concentration decrease is the •OH generation caused by H₂O₂ (in the presence of O₃, H₂O₂ is consumed to produce •OH [67] according to the following

equations (Equations (5) and (6)) and the consumption by the pollutant in aqueous solution and its degradation intermediates:



Therefore, the catalyst effect in the DBD reactor is significant.

Another study demonstrated the synergistic effect of plasma coupled with catalyst in the degradation of Enrofloxacin (EFA). Here the authors used a pulsed discharge plasma (PDP) in which graphene nanocomposites-WO₃ were inserted [68]. In this paper, the authors demonstrated that the presence of nanocatalysts allowed to reach higher EFA removal efficiencies (99% in 60 min of treatment) compared to those obtained with PDP plasma alone (23.1% after the same treatment time). The authors also demonstrated the effect of air flow rate on EFA degradation efficiency in the plasma reactor. In fact, they showed that the EFA degradation efficiency increased with the increase of air flow rate in the reactor up to a certain value, beyond which the degradation efficiency of the contaminant reached a plateau. This result was due to the fact that, with the excess air flow rate, the interaction time of the electric field with the gas molecules is reduced. Furthermore, in this way, the use of reactive species is reduced and the degradation efficiency of the contaminant no longer changes. In order to explore the catalyst mechanism on the EFA degradation in PDP-rGO/WO₃ system, the production of O₃, OH, and H₂O₂ was investigated. It turned out that the catalyst WO₃, excited by plasma, lead to the production of electron-hole pair (e⁻ and h⁺). The generated h⁺ can react with water and produce the hydroxyl radicals. Moreover, the e⁻, transferred from the valence band to conduction band, due to the existence of rGO, can be transferred to the rGO surface. In this case, the generated O₃ by PDP can react with e⁻ on the surface of rGO and produce OH radicals. The proposed catalyst mechanism is reported below in (Equations (7)–(12)):



It was also found that the O₃ produced in the PDP-rGO/WO₃ system after 60 min of treatment was higher than that in the PDP system alone. The rGO/WO₃ addition was beneficial to O₃ generation. This phenomenon was due to the generated h⁺ characterized by a higher oxidizing potential and can react with O^{-•} and O₂^{-•} produced from PDP, leading to O₃ generation [69].

Thus, it is possible to summarize that the self-generated OH radical, O₃, and H₂O₂ by PDP associated with the catalytic generated OH radical and holes by rGO/WO₃, are simultaneously responsible for the decomposition of EFA. However, the decomposition of the EFA molecule leads to the formation of intermediate compounds. In this work, the authors were very precise in identifying the various degradation steps. It emerged that the synergistic effect between plasma and catalyst succeeds in the mineralization of the intermediates.

As regards the recyclability, the catalyst proposed in this work did not lose its performance after four treatment cycles [68].

An interesting study by Guo et al. analyses the property of graphene TiO₂ nanocomposites for synergetic degradation of fluoroquinolone antibiotics (FLU) in a pulsed discharge plasma system [70]. In this work, the authors obtained a hybrid TiO₂-rGO, able to increase the light absorption generated by the plasma. Furthermore, this coupling (TiO₂-graphene) allows a better separation of the electron-hole

pairs with consequent improvement in photocatalytic performances in the PDP system. In particular, it was observed that with the increase of graphene content, the FLU degradation efficiency enhances up to a specific amount of rGO. The presence of an optimal loading of rGO allowed to obtain the highest FLU removal efficiency (99.4%) after 60min of treatment time, which is 23.7% and 34.6% higher than that of PDP/TiO₂ and the PDP alone system, respectively. As regards the stability of this catalyst, it seems to be quite good. In fact, from the XRD analysis performed after four cycles, the spectrum remains unchanged. However, the degradation efficiency seems to slowly worsen (86.4% after four treatment cycles against 99.4% after the first cycle). The role of reactive species was investigated and it was observed that OH[•] and O₂^{-•} play a fundamental role in the FLU degradation in the presence of hybrid TiO₂-graphene [70].

The proposed reaction mechanism is very similar to that proposed in the previously cited work.

Another recent study investigated the degradation of sulfamethoxazole (SMZ) from wastewater by DBD combined with Bi₂WO₆-rMoS₂ [52]. The degradation efficiency of the antimicrobial drug was greatly improved (97.6% compared to 72.5%) with the combined effect of the DBD plasma reactor with Bi₂WO₆-rMoS₂ nanocomposites. In this work, the authors evaluated the effect of oxidizing species by introducing ozone and hydrogen peroxide used as indirect signals of the formation of the [•]OH radicals. In fact, during the plasma discharge [•]OH radicals can be generated by H₂O₂ consumption or by the decomposition of O₃ in alkaline conditions. During the experiments, it was observed that the formation of H₂O₂ was greater in the system “plasma + catalyst” than in the plasma “alone”. In fact, in the combined system, H₂O₂ can be generated through two ways: (1) collision of two hydroxyl radicals [67]; (2) High-energy electron bombard water molecules [71]. In the plasma “alone”, H₂O₂ production depends on the first reaction. In addition, O₃ is a fundamental oxidizing species for the degradation of SMZ in plasma systems. As regards O₃ formation, it was observed that in the combined system (plasma + catalyst), its production was lower than in the plasma “alone”. This effect was mainly due to the photodecomposition of the ozone adsorbed on the surface of the Bi₂WO₆-rMoS₂ photocatalyst [72]. Through identification of the best operating conditions (higher discharge voltage and Bi₂WO₆-rMoS₂ dosage, lower initial concentration and weak alkaline conditions), Zheng et al. highlighted that this catalyst showed good recyclability, even after four cycles of use [52]. The possibility of using a catalyst for several treatment cycles in a plasma reactor is an aspect that should not be underestimated as it is very important for real applications, costs, and from an environmental point of view.

Wang et al. reported the degradation of triclocarban (TCC) in water by dielectric barrier discharge plasma combined with TiO₂/activated carbon fibers (ACFs) [53]. In this work, the authors proposed to insert in a planar DBD reactor the ACFs modified with TiO₂. Once again, the combination of a DBD reactor with catalyst improves the performance of this technology in terms of pollutant degradation. In particular, in this process, the DBD/TiO₂/ACFs combined system allows to adsorb the O₃ generated by the plasma, producing surface free radicals. The combination of the DBD with the catalyst allows to improve the performances of the technology in terms of mineralization of this pharmaceutical compound. Specifically, in the present case, there is an increase of 12% in terms of TCC mineralization and a decrease in its acute toxicity from 64% to 32% after 30 min. Recyclability tests have shown that the TiO₂/ACFs catalysts maintained a high reactivity even after five catalytic cycles.

As for the catalytic mechanism, everything starts from the following reaction:



Meanwhile, water and oxygen molecules were able to transfer electrons from the photocatalyst conduction band and holes from its valence band to produce OH radical via chain reactions:





The authors have conducted a number of experiments with the aim of highlighting the role of these radicals in the TCC degradation process. From the results, it was possible to establish that, in this case, the OH^\bullet played an important role in TCC degradation in the presence of TiO_2/ACFs [53].

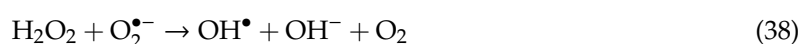
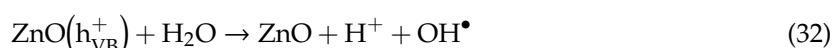
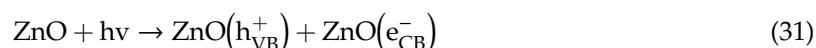
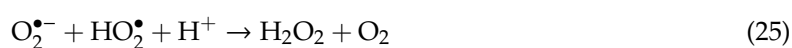
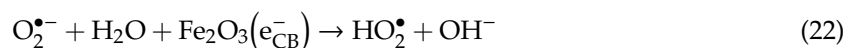
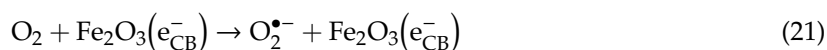
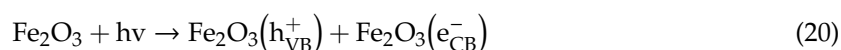
A very similar approach was used for the degradation of triclosan (TCS) belonging to pharmaceuticals and personal care products. In this case, the process provides a DBD reactor combined with activated carbon fibers [54]. In this work, the electric discharge generates plasma which not only can degrade the TCS but also allows in situ regeneration of ACFs and their reuse for different treatment cycles. With respect to the process reported by Jian Wang et al., the degradation and mineralization efficiency are higher at almost the same starting condition (initial pollutant concentration, same reactor) in shorter times, but it is important to point out that the value of the input power is more than double than that used by Jian Wang et al. [53]. Furthermore, by varying the pH of the solution, an improvement or worsening in terms of total organic carbon (TOC) removal was observed. In particular, it was observed that under alkaline conditions, the dissolved O_3 easily decomposed into $\bullet\text{OH}$, while in an acid environment, a greater number of $\bullet\text{OH}$ was produced, allowing faster decomposition of TCS. The recyclability tests carried out for five cycles on the same catalyst sample demonstrate the possibility of reusing the ACFs catalyst without any treatment, thanks to the ability of the plasma to regenerate the activated carbon fibers in situ. In this work, the role of the main oxidizing species responsible for the degradation of the contaminant has not been investigated [54].

Ansari et al. reported the degradation of amoxicillin by the $\text{ZnO}/\alpha\text{-Fe}_2\text{O}_3$ composite catalyst into the NTP-DBD reactor [73]. With this system, the amoxicillin (AMX) degradation rate was equal to 99.3% after 18 min of treatment time, with a voltage of 15 kV, a $\text{ZnO}/\alpha\text{-Fe}_2\text{O}_3$ dosage equal to 0.4 g/L, and AMX initial concentration equal to 16 mg/L and pH of 4.5. In particular, it was possible to observe that the $\text{ZnO}/\alpha\text{-Fe}_2\text{O}_3$ catalyst enhanced the AMX degradation from 75% (using single plasma reactor) to 99.3% (with the optimal condition). In addition, in this case, the catalyst proposed proves to be reusable for several cycles. In particular, the AMX degradation efficiency remains equal to 97.0% even after five reuse cycles. This result indicated that the composite catalyst was stable and reusable in plasma discharge. In this work, a plasma catalysis mechanism was proposed. The authors define that, in the presence of air, plasma alone is capable of generating a population of active species (Reactive Oxygen Species- ROS), ions, and electrons over the liquid surface. These ROS (OH^\bullet , H_2O_2 , O_3 and $\text{O}_2^{\bullet-}$) are known to be able to play a very important role in the degradation of contaminants in water. NTP also form UV light radiations in the wavelength range appropriate for the activation of Fe_2O_3 and ZnO [74,75].

The coupling of ZnO with $\alpha\text{-Fe}_2\text{O}_3$ improves the photocatalytic activity in the presence of UV and visible light. In particular, under UV radiation, the e^- generated in Fe_2O_3 can be inserted into ZnO , and the h^+ created in ZnO can be inserted into Fe_2O_3 . Thus, what mechanism is being observed here? An electron is expected to be excited from the VB to the CB, creating a positive hole in the VB, when the composite catalyst absorbs UV-Vis photons produced during the plasma discharge.

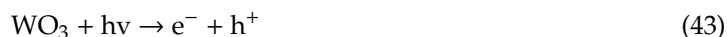
The electrons present in the CB of ZnO move to the surface oxygen and produce O_2^- . Similarly, the holes in the VB of $\alpha\text{-Fe}_2\text{O}_3$ combine with the adsorbed H_2O and hydroxide (OH^-) on the surface of the composite catalyst and generate OH^\bullet radicals. As with the photo-generated reactive species, the active species emitted from the plasma ($\text{O}_2^{\bullet-}$ and OH^\bullet) correspond with the plasma-catalytic pollutant molecules. H^+ ions and OH^\bullet radical degrade organic contaminants. The production of H^+ ions and OH^\bullet radical occurs by H_2O_2 or O_2 , which block the holes present on the surface of the ZnO .

Therefore, Ansari et al. proposed this interesting possible mechanism of catalyst activation in NTP for the AMX degradation [73]:



The degradation of antibiotic chloramphenicol (CAP) in water by pulsed discharge plasma (PDP) combined with TiO_2/WO_3 composites was proposed by Guo et al. [76]. Here, the catalyst was used in powder form and dispersed in the solution to be treated. With this system, the CAP degradation reaches 88% after 60 min of treatment time and with an applied voltage equal to 18 kV. Experiments varying the voltage applied to the system have shown that although an increase in the degradation of the CAP can be found as the voltage value increases, it is also true that only a slight increase in terms of CAP degradation can be observed passing from 18 kV to 20 kV. Therefore, also in this case, it is emphasized that an excessive increase in voltage in order to improve the efficiency of removing the contaminant is actually uneconomical. After each test, the catalyst was recovered and reused for four cycles. The results demonstrated that this catalyst presented the same activity, with only 5% lost after the four cycles of use. Moreover, the XRD analysis performed after each cycle confirmed that there was no significant change between the fresh catalyst and that which was used for four cycles [76]. The experiments carried out in the presence of radical scavengers confirm that, in the presence of a

catalyst in the PDP, OH^\bullet , h^+ and e^- play a crucial role in the catalytic degradation of CAP. Moreover, the results evidenced that $\text{O}_2^{\bullet-}$ has little effect on the catalytic degradation of CAP. In the presence of TiO_2/WO_3 composites, OH^\bullet and h^+ can be generated as follows:



The generated h^+ can react with organic molecules directly or combined with water molecules for further producing the OH radicals.

As regards the O_3 production, also in this work, the results demonstrated that the O_3 concentration declines after the catalyst addition. The explanation of this phenomenon lies in the ability of O_2 and O_3 to capture conduction electrons in TiO_2 , obtaining a consumption of O_2 and O_3 .

Moreover, when the TiW-4 was added, the authors noted that the O_3 concentration was further decreased. Probably, it was because the conduction band level of WO_3 is more positive than the potential of $\text{O}_2^{\bullet-}/\text{O}_2$. This means that the reaction $\text{O}_2 + \text{e}^-_{\text{cb}} \rightarrow \text{O}_2^{\bullet-}$ is not possible in the presence of the TiO_2/WO_3 composite. Therefore, in this case, the conduction electrons present on WO_3 can only be accepted by O_3 , with a consequent higher decomposition rate of the ozone. According to this analysis, the proposed catalytic mechanism by Guo et al. is as follows:

The UV-vis light and electron generated by non-thermal plasma can excite electrons from the valance band (VB) to the conduction band (CB) of TiO_2 and WO_3 , and create holes in the valance band. Since the WO_3 CB is more positive than that of TiO_2 , the generated electrons from TiO_2 CB are easily transferred to WO_3 CB: this prevents the recombination of electrons and holes in TiO_2 . However, because the CB level of WO_3 is more positive than the potential of radical $\text{O}_2^{\bullet-}/\text{O}_2$, the electrons accumulated on the WO_3 CB cannot be captured by O_2 and generate $\text{O}_2^{\bullet-}$. Fortunately, in this case, the generated O_3 by non-thermal plasma can capture the electrons present on WO_3 CB and generate O_3^- , which can further generate OH radicals. Similarly, as TiO_2 VB is more negative than that of WO_3 , the generated h^+ from WO_3 VB can transfer to TiO_2 VB. The h^+ in the TiO_2 VB can react with OH^- or H_2O , and then produces the OH radicals. These new pathways of the photogenerated charge carriers accelerate the electron-hole separation and improve the catalytic performance, with a high degradation of CAP. Thus, in the PDP- TiO_2/WO_3 system, the self-generated OH, O_3 , $\text{O}_2^{\bullet-}$, e^- , due to non-thermal plasma was observed, which can interact on CAP molecules and lead to its decomposition. At the same time, the catalytic generation of OH and h^+ by TiO_2/WO_3 composites can accelerate the decomposition of CAP. In summary, the synergistic actions of PDP and TiO_2/WO_3 catalyst allow the decomposition of the molecule into other by-products, which are, in turn, attacked by the oxidizing species, which transform them into CO_2 and H_2O [76].

Finally, a study investigated by Zhang et al. reported the degradation of acetaminophen (APAP) in gas phase dielectric barrier discharge plasma combined with TiO_2 -rGO nanocomposites [77]. The synergistic effect enhances the APAP degradation from 50% to 92% under 18 kV input voltage. In this work, the authors evaluated the effect of the Graphene Oxide (rGO) amount (wt%) coupled with TiO_2 on the degradation of APAP with NTP, and also the influence of the catalyst dosage. They observed that too high an amount of rGO (wt%) on TiO_2 worsens the performance of the process, in terms of pollutant degradation efficiency. This is probably because a higher amount of rGO results in a decrease in UV absorption catalyst capacity, consequently reducing the exposure of TiO_2 to UV light generated by the plasma itself. As regards the effect of the catalyst dosage on the APAP degradation efficiency,

an improvement in the degradation efficiency of the contaminant was observed as the catalyst dosage increases. However, from an in-depth assessment of energy yield (Y) values (defined as the amount of APAP (g) removed per discharged power (kWh) consumed during the treatment), calculated as reported in Equation (48), it was noted that the energy yield increased significantly, reaching a value of 11.3×10^{-2} g/kWh with a TiO_2 -rGO dosage equal to 0.25 g/L. However, increasing the TiO_2 -rGO dosage at 0.4 g/L, the energy yield value did not increase significantly. Probably the high catalyst dosage (0.4 g/L) led to a high light scattering and reduced the UV transmission, with a consequent reduction in catalytic degradation efficiency.

$$Y = \frac{C_0 \cdot V \cdot K}{P \cdot T} \cdot \frac{1}{1000} \quad (48)$$

where

C_0 (mg/L) is the initial APAP concentration

V (L) is the water volume to be treated

K (%) is the removal rate

P (kW) is the discharge power

T (h) is the degradation time

As regards the recyclability of this catalyst, it has been observed that the plasma is able to decompose the contaminant adsorbed on the surface of TiO_2 -carbon nanocomposites, producing the regeneration of the catalyst and therefore its reuse. However, attention must be paid to the possibility of having a decrease in the functional oxygen groups of TiO_2 -rGO. In fact, from the XPS carried out on this catalyst at the end of each test, a decrease of these functional groups was found. This leads to a reduction in the binding sites for metal oxide, resulting in the lesser amount of attached TiO_2 on rGO sheets and the lowering in photocatalytic activity of TiO_2 -rGO. In fact, as a consequence of this effect, it was noted that after the six-test cycle, degradation efficiency was reduced by 23% compared to the first cycle [77,78]. The following table (Table 1) shows the main characteristics in terms of operating conditions, type of catalyst, and degradation and mineralization efficiency of the contaminants examined in the cited papers.

3.2. Removal of Dyes

Organic dyes represent one of the most significant pollutant groups released into wastewater from textile and other industrial processes. The removal of this kind of pollutant from wastewater represents an important topic from an environmental point of view because of the potential toxicity of the dyes and their visibility in surface waters. The combined effect of NTP with a catalyst appears as a promising technology for the degradation of this kind of pollutant. In the literature, different studies demonstrating the efficiency of the process are reported.

Table 1. Summary of main operating condition and catalyst used for the degradation and mineralization of emerging contaminants in aqueous phase by NTP coupled with catalyst.

| Pollutants | Type of Reactor | Type of Gas | Type of Catalyst | Operating Conditions | Degradation | | Mineralization | | Ref. |
|-------------------------------|-----------------|-----------------|--|----------------------|-----------------------|-----------------------|-----------------------|-----------------------|------|
| | | | | | NTP Alone | NTP + Cat | NTP Alone | NTP + Cat | |
| Levofloxacin (20 mg/L) | DBD | air | Ag ₃ PO ₄ /ACFs (0.490 g/L) | 10 kV pH = 2.69 | 63% after 18 min | 93% after 18 min | 11% after 18 min | 46% after 18 min | [49] |
| Enrofloxacin (20 mg/L) | PDP | air (4 L/min) | graphene-WO ₃ nanocomposites (0.3 g) | 22 kV | 76% after 60 min | 99.1% after 60 min | 31.6% after 60 min | 39.9% after 60 min | [28] |
| Fluoroquinolone (40 mg/L) | PDP | air (4 L/min) | graphene-TiO ₂ (0.2g/L) | 18 kV | 64.8% After 60 min | 99.4% after 60 min | 27.2% after 60 min | 35.8%after 60 min | [70] |
| Sulfamethoxazole (20 mg/L) | DBD | air | Bi ₂ WO ₆ -rMoS ₂ (0.08 g/L) | 9 kV pH = 8.76 | 72.5% after 21 min | 97.6% after 21 min | - | - | [52] |
| Triclocarban (10 mg/L) | DBD | air | TiO ₂ /ACFs | 38 W | 32% after 30 min | 64% after 30 min | 12% after 30 min | 27% after 30 min | [53] |
| Triclosan (10 mg/L) | DBD | Atmospheric air | ACFs | 80W pH = 3.50 | 85% after 18 min | 93% after 18 min | 12% after 18 min | 24% after 18 min | [54] |
| Amoxicillin (16 mg/L) | DBD | air | ZnO/ α -Fe ₂ O ₃ (0.4 g/L) | 15 kV pH = 4.5 | 70% after 18 min | 99.3% after 18 min | 40% after 18 min | 60% after 18 min | [73] |
| Chloramphenicol (20 mg/L) | PDP | air (4 L/min) | TiO ₂ /WO ₃ (0.2 g/L) | 18 kV | 51.3% after 60 min | 88.1% after 60 min | 33.7% after 60 min | 42.5% after 60 min | [76] |
| Acetaminophen (20 mg/L) | DBD | air (3.3 L/min) | TiO ₂ -rGO nanocomposite (0.25 g/L) | 18 kV pH = 7.2 | 50% after 18 min | 92% after 18 min | - | - | [77] |

Liu et al. (2020) showed the efficiency of NTP (DBD reactor) combined with $g\text{-C}_3\text{N}_4/\text{TiO}_2$ for the degradation of Acid Orange 7 dye in aqueous solution. They demonstrate that, by the combination of NTP with $g\text{-C}_3\text{N}_4/\text{TiO}_2$, it was possible to obtain a degradation and mineralization equal to 100% and 57.9%, respectively, after 12 min of treatment [79]. Graphitic carbon nitride ($g\text{-C}_3\text{N}_4$) is a type of semiconductor characterized by excellent physical and chemical stability, used as a catalyst for different purposes such as photocatalytic synthesis, photochemical water splitting, and photocatalytic degradation of organic contaminants under visible light. For this reason, in the literature, the use of this semiconductor is reported in combination with other materials in order to inhibit the recombination of photogenerated electron-hole pair and improve the photocatalytic performance also in presence of visible light [80]. For this type of composite, it is worth underlining that the presence of $g\text{-C}_3\text{N}_4$ in the $g\text{-C}_3\text{N}_4/\text{TiO}_2$ catalyst inhibits the formation of TiO_2 agglomerates, improving the absorption of light and therefore the photocatalytic performance. Furthermore, in the presence of this catalyst, the contribution associated with the adsorption of AO7 was minimal, confirming that the improvement in the degradation of this dye was essentially due to the synergistic action between the plasma and the photocatalyst. Liu et al. observed the influence of operating conditions on the efficiency of the process. They also observed that by increasing the discharge power from 15 to 20 W, the efficiency in terms of AO7 degradation improved significantly, but a further increase from 20 to 25 W led to a worsening in AO7 degradation. In fact, by increasing the power, it is possible to increase the number of oxidizing species such as O_3 , OH^\bullet , and H_2O_2 , thus improving the degradation process of the contaminant. However, the further increase in power discharge leads to a worsening of process performance, probably because an increase in temperature occurs in the area where the electrical discharge occurs, with consequent decomposition of reactive species such as H_2O_2 and O_3 , and therefore a worsening of the degradation of the contaminant [81]. Furthermore, by analyzing the role of the main oxidizing species, it was possible to observe that the fundamental role for the degradation of AO7 in the presence of the $g\text{-C}_3\text{N}_4/\text{TiO}_2$ catalyst is given by superoxide. In particular, h^+ and radical OH^\bullet are also the responsible reactive species in AO7 degradation, but superoxide plays a key role in the degradation of this contaminant in this type of system. The obtained results show that the presence of a catalyst in NTP system is able to define the degradation mechanism of the dye through the production of specific reactive species most responsible for the pollutant degradation [79].

The AO7 degradation is also reported by Guo et al., showing the application of pulsed discharge plasma (PDP) combined with activated carbon (AC) [82]. The presence of AC in the PDP/AC system contributes to creating a synergistic effect, thanks to the adsorbent and catalytic action of the AC. In particular, the effect of AC addition on the production of activated species was studied, especially as regards the formation of OH^\bullet and O^\bullet radical. In detail, from the analysis of the OH^\bullet and O^\bullet emission spectra, it was possible to observe that in the presence of AC in the PDP plasma reactor, the formation of OH^\bullet is significantly increased (the relative emission intensity of OH^\bullet in the PDP/AC system was higher than that in only PDP). However, although the production of hydroxyls species is promoted by the presence of AC, the removal of TOC is limited. Analyzing the data reported in this paper, it is in fact possible to note that the TOC removal was equal to about 27%. Since organic carbon is still present in the solution, it is evident that the oxidizing species promoted by the presence of AC are able to attack the azoic double bond ($-\text{N}=\text{N}-$) responsible for the color, but unable to destroy the aromatic rings generated during the AO7 degradation process [82]. This aspect should not be underestimated since by applying an advanced oxidation process, it is desirable to obtain the complete (or almost) mineralization of the organic substance present in the solution. Probably in this specific case, it may be necessary to evaluate the improvement in the operating parameters involved (voltage, gas flow rate, type of process gas) or to provide the presence of other specific processes after the NTP oxidation necessary for the removal of byproducts.

As regards the application of activated carbon fibers, Zhang et al. proposed their use combined with TiO_2 [83]. Specifically, in their work, they report the use of activated carbon fiber loaded with TiO_2 for the degradation of methyl orange (MO) in aqueous solution using a PDP reactor.

In their reactor configuration, a very high input voltage (46 kV) and oxygen flow rate equal to 90 L/h (1.5 L/min) were used. It has been observed that the concentration of the MO decreased, thanks to the adsorbing action of the AC/TiO₂ alone. On also applying electric discharge, it was possible to notice an improvement in terms of MO degradation. Furthermore, the adsorbing capacity of this composite seems to be quite high even after five treatment cycles, confirming that, also in this case, the plasma is able to regenerate the catalytic filling material. Specifically, the AC seems to play an adsorbent role while TiO₂ plays a photocatalytic role, absorbing the UV light produced by the plasma and favoring the transformation of O₃ into OH• radicals, which increase the degradation of MO and the reaction by-products. In this paper, an interesting observation was made about the influence of solution conductivity on COD (chemical oxygen demand) removal. The solution's conductivity changes according to the presence of by-products in the solution. In fact, it was observed that in the case of PDP alone, the ozone produced leads to the formation of by-products (aldehydes and organic acids), which led to pH and conductivity decrease. In the presence of PDP combined with the AC/TiO₂ action, it was possible to observe the by-product mineralization to H₂O and CO₂; simultaneously an increase in the solution pH and a decrease in the conductivity was observed. Obviously, these results lead to an increase in COD removal. Specific analyses to evaluate the effect of conductivity on COD removal were carried out, and they showed that COD removal decreased with increased solution conductivity [83].

Iervolino et al. reported the degradation of acid orange 7 dye (AO7) in aqueous solution using Fe₂O₃ as a catalyst immobilized on glass spheres, in a DBD reactor [18]. The authors show that the use of catalytic packed material allows to obtain the complete degradation of AO7 pollutant in a very short time (10 min) with an applied voltage equal to 12 kV, lower than those generally used for this technology. The presence of a packed material, catalytic or not (such as glass spheres alone), is confirmed as important in improving the performance of the NTP process generated by a DBD reactor. The some authors confirm that the presence of packed material can improve the distribution of the electric field, or even create intense micro-discharges at the surface and at the corners of the material inserted in the reactor [61]. Another important aspect to be considered in this work is the absence of reaction by-products, as demonstrated by HPLC analysis. Thus, with this system, it is possible to obtain the complete mineralization of AO7 dye in aqueous solution. Moreover, as regards catalyst recyclability, it was shown that even after several cycles, the catalyst did not present substantial performance decreases [18]. They also investigate the role of the main reactive species and it emerged that, in the presence of Fe₂O₃ catalyst in the DBD reactor, the main oxidizing species was represented by O₂•⁻. Without the Fe₂O₃ catalyst, but in the presence of the only glass spheres, the AO7 degradation was promoted both by the O₂•⁻ and the hydroxyl radicals. This indicates that, in the last case, there was not one single oxidizing species most responsible for the pollutants' degradation, but two (O₂•⁻ and •OH). This result depends on the type of catalyst and it allows to establish the optimal conditions of the process in order to avoid the inhibition of the pollutants' degradation by any radical scavenger present in the water to be treated [18].

Additionally, the degradation of crystal violet dye in aqueous solution by DBD coupled with BiPO₄ has been reported [84]. This catalyst did not demonstrate adsorption of the CV dye, but it acts in the photogeneration of reactive species. In fact, its presence in the DBD reactor allowed to increase the degradation of the dye up to 28% after 12 min of treatment. In addition, in this case, it has been observed that an increase in input power causes improvements in terms of dye degradation, up to a certain power value, beyond which a worsening in the degradation efficiency of the dye was observed. As in the previous cases, also in this work, it has been emphasized that too high a power value can cause a temperature increase, which might lead to the decomposition of the generated oxidizing species. It is also interesting to underline another aspect: the possible formation of NO_x. When power increases beyond a certain value, NO_x production can also increase through nitrogen oxidation. This means that in this way, reactive oxygen species are consumed, reducing the oxidizing species necessary for the degradation of the contaminant [85].

The degradation efficiency of “Reactive Yellow 176” dye by DBD plasma combining with nano-TiO₂ was reported by Shen et al. [86]. In this work, the initial dye concentration was very high, equal to 200 mg/L, the treated solution volume was 10 mL, and the power supply was 70W. For each experiment, 0.1 g of TiO₂ photocatalyst was placed in RY176 aqueous solutions and the process gas used was atmospheric air. From the results, it was observed that the dye degradation efficiency was equal to 83.54%, which was 17.33% higher than that obtained by only DBD plasma under the same operation condition. In particular, COD removal was equal to 70% after 3 min of treatment time. An interesting parameter considered in this work is that the energy consumption estimated was about 5.27×10^6 J/g in order to obtain the COD removal equal to 70%. This energy consumption value corresponds, considering the price of electricity reported by the authors, to an electricity cost for treatment equal to 22.9 \$/ton. This data is important as it also allows to make an evaluation of the process from an economic point of view, which is difficult to find in other scientific articles.

In addition to the use of the DBD reactor which, as reported in the previous paper, seems to be the most used configuration when the NTP was coupled to the catalyst activity, in the literature, the use of the plasma obtained through the gliding arc reactor, coupled with a particular catalyst, the laterite soil, is reported [65]. Laterite is a mixture of ferric hydroxide, aluminum hydroxide, titanium, rarely manganese and free silica, and its use as a catalyst combined with gliding arc plasma for the Orange G (OG) degradation in aqueous solution is reported [65]. In this system, the use of a laterite aqueous suspension prepared by adding the appropriate amount of catalyst to the aqueous solution of OG was provided. The solution was kept under dark conditions for 20 min in order to evaluate the possible adsorption of the contaminant on the catalyst surface. At this point, the gliding arch system was placed over the suspension kept stirred by a magnet. During the tests, the authors observed that an important parameter that influences the catalyst performance in the gliding arc reactor is the calcination temperature. In fact, in the case of non-calcined laterite, the catalytic sites could be covered by impurities that are instead eliminated during the calcination process. Moreover, after calcination, laterite is more crystalline and therefore is characterized by better catalytic activity. Using the right catalyst load, it was possible to observe that the presence of laterite favors the formation of OH radicals generated by the decomposition of H₂O₂ with the iron species (this is very similar to a “Fenton” reaction) present on the laterite surface. The presence of a catalyst, in suitable amounts, allows for a better hole photogeneration and thereby of OH• radical. Recyclability tests have also shown that laterite is not only an efficient catalyst for the oxidation of OG in non-thermal plasma conditions but also a relatively stable catalyst. Therefore, in the presence of laterite in an NTP reactor, the OG degradation was mainly promoted by OH radicals, as confirmed by the experiment in the presence of OH scavenger [65]. The main parameters of the process reported below are summarized in Table 2.

3.3. Decontamination of Organic Pollutants Different from Pharmaceuticals and Dyes

The degradation of other kinds of organic pollutants (not pharmaceutical or dyes) by catalytic NTP is reported in the literature.

Ahmad et al. investigated the efficiency of two catalysts, α -Fe₂O₃-TiO₂ and persulfate (Na₂S₂O₈), to improve the performance of the NTP process, obtained through a DBD-type reactor, for the degradation of dimethyl phthalate (DMP) in aqueous solution. DMP is a kind of pollutant generally present in plastic industrial wastewater, and can be considered as an endocrine-disrupting compound. In this system, under optimal operating conditions (applied voltage 4 kV, pH equal to 3, persulfate concentration of 2 mM/L and nanocomposite concentration of 1 g·L⁻¹), the 100% of DMP was degraded after only 5.2 min of reaction time. As possibly observed, to obtain very high degradation efficiency, it is necessary to modify the pH of the solution. In fact, the type, role, and amount of reactive species and also of the sulfate radical depend on pH value [87].

Table 2. Summary of the main operating condition and catalyst used for the degradation and mineralization of dyes in aqueous phase by NTP coupled with catalyst.

| Pollutants | Type of Reactor | Type of Gas | Type of Catalyst | Operating Conditions | Degradation | | Mineralization | | Ref. |
|--------------------------------|-----------------|------------------------------|--|----------------------|------------------------|------------------------|--------------------|--------------------|------|
| | | | | | NTP Alone | NTP + Cat | NTP Alone | NTP + Cat | |
| Acid Orange7 (5 mg/L) | DBD | air (0.014 L/min) | g-C ₃ N ₄ /TiO ₂ (0.5 g/L) | 20 W pH = 10 | 61% after 12 min | 100% after 12 min | 5.6% in 12 min | 57.9% in 12 min | [79] |
| Acid Orange7 (50 mg/L) | PDP | O ₂ (4 L/min) | Activated carbon (4 g) | 20 kV pH = 7 | About 58% after 60 min | About 83% after 60 min | 19.8% after 60 min | 30.3% after 60 min | [82] |
| Acid Orange (20 mg/L) | DBD | O ₂ (0.18 NL/min) | Fe ₂ O ₃ immobilized on glass spheres (36 g) | 12 kV | 14% after 30 min | 80% after 5 min | 8% after 30 min | 80% after 5 min | [18] |
| Methyl orange (80 mg/L) | PDP | O ₂ | ACF/TiO ₂ | 46 kV pH = 4 | 63% after 15 min | 98.2% after 15 min | 56.7% after 15 min | 92.5% After 15 min | [83] |
| Crystal violet (40 mg/L) | DBD | air (1.33 L/min) | BiPO ₄ (0.03g) | 40 W pH = 4.03 | 63% after 12 min | 91% after 12 min | - | - | [84] |
| Reactive Yellow 176 (200 mg/L) | DBD | Atmospheric air | TiO ₂ (0.1g) | 70 W pH = 6.8 | 66.21% after 180 min | 83.54% after 180 min | - | - | [86] |
| Orange G (23 mg/L) | GAD | Air (13.3 L/min) | Laterite soil (3 g/L) | 10 kV pH = 3 | 17% after 60 min | 100% After 60 min | - | 83% After 60 min | [65] |

Nian et al. investigated the role of methylparaben by DBD reactor combining with ZnO-rGO. In this case, complete degradation of the pollutant is obtained in a few min at 20 W. During the process, many intermediate compounds are formed, which cannot be completely degraded. This is the reason why very low mineralization values are obtained [75]. An interesting evaluation carried out by the authors in this work is about the economic point of view. The authors report a comparison between the energy yield (expressed as: $Y = \text{g/kW h}$) (the cost) of NTP technology for the removal of methylparaben, phenol, or bisphenol A, and which of the other technologies are based on advanced oxidation processes (AOPs), such as photocatalysis, ultrasound, Fenton, and electro-Fenton. This study shows that, thanks also to the presence of the ZnO-rGO catalyst, NTP technology is the one that guarantees higher values in terms of energy efficiency and therefore lower costs. Furthermore, in accordance with other studies [1,18], the highest energy yield with NTP is obtained in the presence of a high initial concentration of contaminant in aqueous solution. This aspect underlines that NTP, coupled with the catalyst, is able to produce a high number of oxidizing species, which can be used in particular conditions (high concentrations of contaminants) and in the presence of pollutants difficult to degrade [75].

Another organic compound that has attracted the attention of the scientific community is bisphenol A, which is used to synthesize polymer materials, such as polycarbonate and epoxy resin, and is also an important component for the manufacturing of plasticizers, flame retardants, heat stabilizers, pesticides, coatings, and other fine chemical products. Yan et al. reported the use of nano-zinc oxide for the removal of Bisphenol A (BPA) from aqueous solutions using a DBD plasma reactor. With an applied voltage equal to 5 kV (this value is lower with respect other literature data) and in the presence of air flow rate equal to 0.5 L/min, the degradation efficiency of BPA (20 mg/L of initial concentration) reached 85.4% in the presence of nano-ZnO (catalyst dosage equal to 50 mg/L) in the DBD system, which was 17% higher than that of the BPA degradation in the DBD alone. In this study, the authors also paid particular attention to the process gas used during the experiment. They compared DBD-nano-ZnO performances in the presence of O_2 and air. The best results, summarized in Table 3, underlined that bubbling oxygen in the DBD reactor makes it possible to generate more active species. Oxygen atoms could be excited, dissociated, and collided to produce O_3 . On applying the electric discharge to a gas consisting of O_2 , the production of O_3 is favoured. Consequently, the formation of OH^\bullet radicals and other oxidizing species is also enhanced, thus leading to a more efficient degradation of pollutants [88]. The same hazardous pollutant (BPA) at the same initial concentration was studied by Guo et al. [89]. In this case, a pulsed discharge plasma (PDP) reactor was used, and the activated granular carbon (GAC), used as a catalyst, was put on the stainless steel plate used as ground electrode. Air was used as process gas in the PDP reactor. The GAC amount that is used in the system is important as it can improve NTP performance. In fact, its presence contributes to an increase in active species. However, even in this case, a higher amount of catalyst can lead to a worsening of process performance. In the specific case of GAC, presented in this paper by Guo et al., it was observed that a higher GAC amount can create agglomerates, which decrease its contact area with the contaminant molecules and therefore worsen its catalytic performance. Moreover, at fixed values of input power, and with a defined air flow rate blown into the reactor, the O_3 generated remains constant, and consequently no increase in the radical OH^\bullet species is found. It should also be emphasized that GAC is an efficient adsorbent, able to remove even by itself a high percentage of contaminants from aqueous solutions. For this reason, the control tests are essential to establish the role of each single effect (plasma, adsorption (catalyst), plasma + catalyst) on the degradation of BPA, and therefore the synergistic effect of these on the total degradation of pollutant. The authors of this work performed this important evaluation by several experiments: GAC alone, plasma alone, and PDP with GAC. The synergistic effect is confirmed by the fact that in the presence of materials with a high surface area such as GAC, the oxidizing species (O_3) and contaminants present in water are easily adsorbed on the surface of this material. In this way, the OH^\bullet radicals production is favored, also increasing the degradation of its intermediate compounds. Moreover, experiments in the presence of radical scavengers were carried out. The results confirmed that the main reactive species most responsible for BPA degradation in PDP+ GAC are the OH^\bullet radicals.

This suggested that GAC addition is selective in the formation of OH• radicals. Finally, a result already discussed previously, which concerns the possibility of regenerating the adsorbent material in situ, was also reported in this work. In particular, it has been shown that during the test, after 60 min of treatment, the GAC can be regenerated by PDP treatment, and it can be used to increase the BPA degradation at the same time [89].

Table 3. Summary of the main operating condition and catalyst used for the degradation and mineralization of other organic pollutants in aqueous phase by NTP coupled with a catalyst.

| Pollutant | Type of Reactor | Type of Gas | Type of Catalyst | Operating Conditions | Degradation | | Mineralization | | Ref. |
|-------------------------------------|-----------------|---|---|----------------------------|------------------------|-----------------------|-----------------------|-----------------------|------|
| | | | | | NTP Alone | NTP + Cat. | NTP Alone | NTP + Cat | |
| Dimethyl phthalate (DMP) (100 mg/L) | DBD | air (0.5 L/min) argon (4.5 L/min) | Fe ₂ O ₃ -TiO ₂ (1 g/L) with Na ₂ S ₂ O ₈ | 14 kV pH = 3 | 100% after 24.6 min | 100% after 5.2 min | - | - | [87] |
| Methyl paraben (20 mg/L) | DBD | air (0.33 L/min) | ZnO-rGO nanosheets (0.015 g/L) | 20 W pH = 7.0 | 55% after 15 min | 99% after 15 min | - | 10% after 15 min | [75] |
| Bisphenol A (20 mg/L) | DBD | O ₂ (0.5 L/min) | nano-ZnO (50 mg/L) | 5 kV pH = 2 | 68.4% after 20 min | 100% after 20 min | 46.9% after 40 min | 50% after 40 min | [88] |
| Bisphenol A (20 mg/L) | PDP | Air (4 L/min) | GAC (4g) | 20 kV acidic conditions | 68.4% after 60 min | 98.7% after 60 min | 23.3% after 60 min | 34.6% after 60 min | [89] |
| Ammonia nitrogen (50 mg/L) | Not reported | O ₂ (1 L/min) | Zeolites (2 g) | 2.2. kV pH = 6.18 | 8.42% after 30 min | 69.9% after 30 min | - | - | [90] |
| Caffeine (50 mg/L) | DBD | dry air, O ₂ , N ₂ and Ar (0.4 L/min) | Goethite (2.5 g/L) | 75 W pH = 7 | 41% after 24 min | 94% after 24 min | 12% after 24 min | 20% after 24 min | [91] |

Non-thermal plasma combined with zeolites was used to remove inorganic pollutant ammonia nitrogen from wastewater. This study was reported by Fan et al. In this paper, the authors did not classify the type of reactor, but according to how it was described (“the plasma reactor consists of a plexiglass cylinder, two hollow stainless steel needles and a stainless-steel plate”), it could be considered as a PDP reactor. From the results, it can be observed that after 30 min of reaction time, the ammonia nitrogen removal efficiency was 8.42% for the plasma alone, 53.74% in the case of adsorption due to sole zeolite and 69.97% for the plasma + zeolites process. It is important to underline that the removal efficiency of the contaminant in the combined plasma + zeolites system is greater than the sum of that in the plasma alone and sole zeolites adsorption. This confirmed that the combination of plasma and zeolites had a synergistic effect. Thanks to the presence of zeolite, it is possible to catalyze the transformation of O₃ and H₂O₂ produced during the discharge, in other species such as the OH• radicals that allow a greater removal of ammonia nitrogen. It is interesting to observe that to obtain a good degradation of ammonia nitrogen in the combined plasma + zeolites system, very low voltage input values are sufficient (2.2 kV with 14 kHz). As was also observed in previous works, the increase in input voltage slightly improves the % of degradation and therefore the efficiency of the system. This means that a high input energy aggravates the energy consumption of the system, also bringing instability to the reaction [90].

Another recent study demonstrates the efficiency of goethite as a catalyst into DBD reactor for the degradation of caffeine [91]. Caffeine is a widely used stimulant, present in various types of drinks. Its presence has been detected in many surface and underground waters due to the low efficiency of conventional water treatments in degrading this type of substance [92]. In this work, the authors describe well the presence of goethite, in powder form, which is positioned in the discharge zone of the reactor, in direct contact with the plasma discharge. From the experimental results, it was possible to note that this combined system exhibited excellent performance in terms of caffeine removal (94% of degradation after 18 min of treatment) and energy efficiency. However, with respect to the other catalytic material, in the presence of goethite alone, no caffeine degradation was observed. The presence

of goethite accelerates the decomposition of O₃ in other oxidizing species such as hydroxyl radicals, which are able to degrade caffeine and its reaction by-products. Furthermore, goethite is characterized by a band gap equal to 2.1 eV; it is, therefore, able to absorb the light emitted by the plasma and act as a photocatalyst. As regards the role of the main reactive species, the authors indicate that OH• plays an important role in the caffeine degradation in the goethite + DBD system. However, it should be emphasized that in this system, the total mineralization of caffeine is not guaranteed: only 20% of caffeine is mineralized to CO₂ and H₂O. As regards the recyclability tests, it was demonstrated that goethite is a stable catalyst in the DBD reactor [91].

4. Economic Evaluation

The economic aspect is certainly one of the key parameters for application of non-thermal plasma treatment. The most important economic indicator for the evaluation of process performances could be defined by energy yield calculates, as reported in Equation (49).

In general, from literature studies, it was evident that energy yield in the catalytic/NTP processes was much higher compared to NTP alone. Furthermore, the addition of a catalyst combined with the NTP system can contribute to the economic stability and sustainability of this system in environmental applications.

Once the energy yield is defined, it is possible to estimate the operational cost as:

$$E \text{ (operational cost)} (\$/g) = \frac{X \text{ unit price of electrical energy } (\$/\text{kWh})}{\text{energy yield } \left(\frac{g}{\text{kWh}}\right)} \quad (49)$$

From the literature, it was found that the energy yield depends mostly on the initial concentration of pollutants, type of plasma reactor, characteristics of NTP reactor, and addition of a catalyst [93]. An interesting study reports the analysis cost of NTP combined with ZnO-rGO nanosheets for methylparaben degradation [75]. In particular, the authors compared the costs of current technology with other advanced oxidation processes like ultrasonic technology or photocatalysis. The main results obtained from this research are summarized in Table 4.

From the collected data, it has emerged that the operational costs of the photocatalytic process and of ultrasonic technology were much higher than those of the NTP/catalyst system, despite the cost of Fenton or electro-Fenton being lower. Generally, the NTP process is a cost-effective decontamination technique, as compared to several other conventional techniques. The key factors to consider are: the cost of plasma gas sources, electricity, and plasma equipment. In the following example (Table 5), the authors compared the NTP cost process as a function of different kinds of gas for fixed operating conditions for a 1000 h operation at 300–2400 m³/h [94].

The use of air as a plasma gas source is the most convenient in term of costs. In the case of He, it is a gas readily ionized compared to others, determining a reduced amount of electricity consumed for the ionization process and the overall power supply cost. The power consumption also depends on the size and gap between the electrodes. In general, from the literature, it is reported that power consumption would be at least two-fold when the NTP process is scaled-up from lab-scale to industrial-scale. A recent study conducted by Sang et al. show that the electricity costs for N,N-dimethylformamide degradation using a DBD reactor are about 0.11 Euro/kWh, with optimal energy efficiency of 13.2 mg/kJ [95]. In conclusion, it is possible to say that real-scale operation cost assessment supports the industrialization of an NTP/catalyst system. Therefore, future works should be conducted for economic evaluations such as energy consumption costs and reactor investment costs.

Table 4. Economic evaluation of the main AOPs for degradation of different organic pollutants in water.

| AOPs | Target Pollutant | Energy Yield Y (g/kW h) | Operational Cost E (\$/g) | Experimental Conditions |
|----------------------------------|------------------|-------------------------|---------------------------|---|
| DBD plasma combined with ZnO-rGO | methylparaben | 0.80 | 0.119 | $C_0 = 2 \text{ mg/L}$ $C_0 = 10 \text{ mg/L}$ $C_0 = 20 \text{ mg/L}$ $\text{pH} = 7.0$, ZnO-rGO dosage = 0.015 g/L, $P = 20 \text{ W}$, $V = 200 \text{ mL}$, $t = 15 \text{ min}$ |
| | | 3.99 | 0.024 | |
| | | 7.98 | 0.012 | |
| photocatalysis | methylparaben | 9.5×10^{-4} | 100.000 | TiO_2 dosage = 2 g/L, $C_0 = 10 \text{ mg/L}$, $\text{pH} = 6.0$, $V = 25 \text{ mL}$, $P = 125 \text{ W}$ |
| photocatalysis | ethylparaben | 3.6×10^{-4} | 263.889 | $C_0 = 0.3 \text{ mg/L}$, $t = 60 \text{ min}$ $C_0 = 0.6 \text{ mg/L}$, $t = 90 \text{ min}$ $C_0 = 0.15 \text{ mg/L}$, $t = 60 \text{ min}$ $P = 100 \text{ W}$, $V = 120 \text{ mL}$ |
| | | 4.8×10^{-4} | 197.917 | |
| | | 1.8×10^{-4} | 527.778 | |
| ultrasonic technology | methylparaben | 1.4×10^{-4} | 678.571 | $P = 7 \text{ W/mL}$, $t = 90 \text{ min}$ $P = 22.75 \text{ W/mL}$, $t = 60 \text{ min}$ $P = 40.25 \text{ W/mL}$, $t = 30 \text{ min}$ $C_0 = 1.52 \text{ mg/L}$, $\text{pH} = 4.6$ |
| | | 6.7×10^{-5} | 1417.910 | |
| | | 7.6×10^{-5} | 1250.000 | |
| ultrasonic technology | bisphenol A | 8.0×10^{-6} | 11875.000 | $P = 100 \text{ W}$ $P = 200 \text{ W}$ $P = 300 \text{ W}$ $C_0 = 0.1 \text{ mg/L}$, $\text{pH} = 6.5$, $V = 50 \text{ mL}$ |
| | | 5.4×10^{-6} | 17399.267 | |
| | | 4.1×10^{-6} | 23171.732 | |
| electro-Fenton | phenol | - | 1.003×10^{-3} | $C_0 = 250 \text{ mg/L}$, current density = 1 mA/cm ² , $\text{pH} = 3.0$, $\text{H}_2\text{O}_2 = 500 \text{ mg/L}$, $\text{Fe}^{2+} = 30 \text{ mg/L}$ |
| Fenton | phenol | - | 1.337×10^{-3} | $C_0 = 250 \text{ mg/L}$, $\text{pH} = 3.0$, $\text{H}_2\text{O}_2 = 500 \text{ mg/L}$, $\text{Fe}^{2+} = 30 \text{ mg/L}$ |

Table 5. NTP cost process as a function of different kinds of gas.

| Gas Process | Costs |
|----------------|-----------------------|
| He | \$636,000–\$9,096,000 |
| N ₂ | \$9000–\$72,000 |
| O ₂ | \$18,000–\$144,000 |
| air | ~\$0 |

5. Future Perspectives

From the data collected in this review, it is evident that the NTP process combined with the use of catalysts is developing quickly. Its application concerns the degradation of different types of contaminants and significant advancement have been made to optimize the operating conditions of this process. However, there are still some issues to be considered in-depth.

For example, it was reported that NTP plays an important role in pollutant degradation. However, techniques for the analysis of internal plasma parameters (such as electron temperature, electron density, ion density, and radical density) should be improved to further understand the removal mechanism inside the plasma reactor. Moreover, the configuration and optimal parameters of plasma reactors should be further investigated in order to improve the interaction between the plasma and the catalyst and, consequently, its regeneration in situ. More detailed studies on the ability of the plasma discharge to influence the catalytic phenomena and the physical and chemical properties of catalysts are also needed. Although it has been stated by many literature studies that the combined NTP + catalyst technology reduces the production of reaction by-products, which can often be formed with other oxidation processes, it is clear that their monitoring must not be neglected in any way. The percentage of degradation of the primary contaminant cannot be the only criteria for evaluating the performance of this process. The possible presence of reaction by-products must be evaluated and this requires the use of suitable analytical tools and techniques. Eventually, it is clear that the operating costs limit the development of catalytic NTP process at an industrial level.

For this reason, the evaluation of operating costs is a fundamental step for the industrialization of a process. Therefore, future works should be carried out focusing on the economic evaluation of this process, which is linked to the energy consumption and investment costs that, in turn, will depend on the type of chosen reactor.

6. Conclusions

The NTP coupled with catalyst technology is a promising approach for the removal of water pollutants. In comparison with NTP alone or heterogeneous catalysis alone, the combination of NTP with heterogeneous catalysts allows better performance. With regards to the reactor configuration, the DBD type seems to be the most used when the catalyst is coupled to the NTP process. Probably, the reason of this choice lies in the fact that DBD configuration allows suitable positioning of the catalyst very close to the discharge zone. In this way, not only is the interaction between the electric field and the catalyst surface better, but the interaction between the UV rays generated by the plasma and its oxidizing species with those generated by the catalyst is also enhanced. Therefore, it is evident that this configuration may not be suitable if a powder catalyst is used. This could be seen as a limiting aspect for the technology. However, the ideal solution could be the use of a structured catalyst. This is an advantageous choice for two reasons: the first, that of guaranteeing the optimal arrangement of the catalyst, which would be “blocked” in the discharge zone; the second relates to the possibility of easily separating the catalyst at the end of the treatment and being able to reuse it for different process cycles.

From the studies reported in this review, a very interesting aspect emerges about the energy yield of this process (NTP with a catalyst). In fact, it has been noted that by increasing the input voltage, improvements in terms of degradation efficiency are not always observed, or perhaps such improvements are not so evident as to justify the use of such a high input voltage. A “waste” of energy

can be observed, therefore of oxidizing species generated with high input voltages, which makes the process, as a whole, not economically convenient. Furthermore, comparing the energy efficiency between NTP and NTP coupled with a catalyst, it can be stated that adding a catalyst in the DBD reactor could help make the process economically sustainable.

It is interesting to note that the non-thermal plasma is able to regenerate the catalyst inserted in the reactor. This aspect is very important as it allows the use of the catalyst for different process cycles and also avoids the use of additional technologies necessary to regenerate the materials used, especially those characterized by a strong adsorbing capacity. Moreover, the presence of the catalyst in the NTP process can influence the role of the oxidizing species most responsible for the degradation of the contaminant, but above all, it is able to avoid the formation of unwanted reaction by-products.

Moreover, it is worthwhile to note that compared with other AOPs, NTP combined with catalysts needed to shorter reaction time, resulting in a higher reactive species production.

Thus, it is possible to confirm, from a wide range of papers, that this novel technique results in a synergistic effect (i.e., the performance achieved for emerging pollutant degradation with plasma catalysis is better than the combination of plasma-alone and catalysis-alone). Furthermore, the presence of a catalyst allows to overcome some limitations in industrial applications since it is able to regulate selectivity towards the desired products.

Author Contributions: Conceptualization G.I., and M.R.; formal analysis, M.R.; investigation, G.I. and M.R.; data curation, V.V. and V.P.; writing—original draft preparation, M.R.; writing—review and editing, G.I.; visualization, V.V.; supervision, V.P. All authors have read and agreed to the published version of the manuscript.

Funding: This research received no external funding.

Conflicts of Interest: The authors declare no conflict of interest.

References

1. Iervolino, G.; Vaiano, V.; Palma, V. Enhanced removal of water pollutants by dielectric barrier discharge non-thermal plasma reactor. *Sep. Purif. Technol.* **2019**, *215*, 155–162. [[CrossRef](#)]
2. Hashim, S.A.; Binti Samsudin, F.N.D.; San Wong, C.; Bakar, K.A.; Yap, S.L.; Zin, M.F.M. Non-thermal plasma for air and water remediation. *Arch. Biochem. Biophys.* **2016**, *605*, 34–40. [[CrossRef](#)] [[PubMed](#)]
3. Shanker, U.; Rani, M.; Jassal, V. Degradation of hazardous organic dyes in water by nanomaterials. *Environ. Chem. Lett.* **2017**, *15*, 623–642. [[CrossRef](#)]
4. Anandan, S.; Kathiravan, K.; Murugesan, V.; Ikuma, Y. Anionic (IO₃⁻) non-metal doped TiO₂ nanoparticles for the photocatalytic degradation of hazardous pollutant in water. *Catal. Commun.* **2009**, *10*, 1014–1019. [[CrossRef](#)]
5. Buttiglieri, G.; Knepper, T. Removal of emerging contaminants in wastewater treatment: Conventional activated sludge treatment. In *Emerging Contaminants from Industrial and Municipal Waste*; Springer: Berlin/Heidelberg, Germany, 2007; pp. 1–35.
6. Rajasulochana, P.; Preethy, V. Comparison on efficiency of various techniques in treatment of waste and sewage water—A comprehensive review. *Resour. Effic. Technol.* **2016**, *2*, 175–184. [[CrossRef](#)]
7. Iervolino, G.; Zammit, I.; Vaiano, V.; Rizzo, L. Limitations and Prospects for Wastewater Treatment by UV and Visible-Light-Active Heterogeneous Photocatalysis: A Critical Review. *Top. Curr. Chem.* **2020**, *378*, 7. [[CrossRef](#)]
8. Liao, X.; Liu, D.; Xiang, Q.; Ahn, J.; Chen, S.; Ye, X.; Ding, T. Inactivation mechanisms of non-thermal plasma on microbes: A review. *Food Control* **2017**, *75*, 83–91. [[CrossRef](#)]
9. Grill, A. *Cold Plasma Generation*; Wiley-IEEE Press: New York, NY, USA, 1994; pp. 24–45.
10. Rossnagel, S.; Cuomo, J.; Westwood, W. *Handbook of Plasma Processing Technology*; Noyes Publications: Park Ridge, IL, USA, 1990.
11. Rutscher, A.; Deutsch, H.-J. *Wissensspeicher Plasmatechnik*; VEB Fachbuchverlag: Leipzig, Germany, 1983.
12. Fridman, A. *Plasma Chemistry*; Cambridge University Press: Cambridge, UK, 2008.
13. Penetrante, M. Plasma-Chemistry and Power Consumption in Non-Thermal Plasma DeNO_x. *Nonthermal Plasma Tech. Pollut. Control* **1993**, 65–90.

14. Jawaharraj, K.; Shrestha, N.; Chilkoor, G.; Dhiman, S.S.; Islam, J.; Gadhamshetty, V. Valorization of Methane from Environmental Engineering Applications: A Critical Review. *Water Res.* **2020**, *187*, 116400. [[CrossRef](#)]
15. Kasih, T.P.; Kharisma, A.; Perdana, M.K.; Murphiyanto, R.D.J. Development of non-thermal plasma jet and its potential application for color degradation of organic pollutant in wastewater treatment. In Proceedings of the IOP Conference Series: Earth and Environmental Science, Yogyakarta, Indonesia, 14–15 November 2017; IOP Publishing: Bristol, UK, 2017; p. 012004.
16. Ceriani, E.; Marotta, E.; Shapoval, V.; Favaro, G.; Paradisi, C. Complete mineralization of organic pollutants in water by treatment with air non-thermal plasma. *Chem. Eng. J.* **2018**, *337*, 567–575. [[CrossRef](#)]
17. Aziz, K.H.H.; Miessner, H.; Mahyar, A.; Mueller, S.; Kalass, D.; Moeller, D.; Omer, K.M. Removal of dichloroacetic acid from aqueous solution using non-thermal plasma generated by dielectric barrier discharge and nano-pulse corona discharge. *Sep. Purif. Technol.* **2019**, *216*, 51–57. [[CrossRef](#)]
18. Iervolino, G.; Vaiano, V.; Pepe, G.; Campiglia, P.; Palma, V. Degradation of Acid Orange 7 Azo Dye in Aqueous Solution by a Catalytic-Assisted, Non-Thermal Plasma Process. *Catalysts* **2020**, *10*, 888. [[CrossRef](#)]
19. Neyts, E.C.; Ostrikov, K.; Sunkara, M.K.; Bogaerts, A. Plasma catalysis: Synergistic effects at the nanoscale. *Chem. Rev.* **2015**, *115*, 13408–13446. [[CrossRef](#)] [[PubMed](#)]
20. Liang, W.; Sun, H.; Shi, X.; Zhu, Y. Abatement of Toluene by Reverse-Flow Nonthermal Plasma Reactor Coupled with Catalyst. *Catalysts* **2020**, *10*, 511. [[CrossRef](#)]
21. Zhu, T.; Zhang, X.; Niu, W.; Liu, Y.; Yuan, B.; Li, Z.; Liu, H. Selective Catalytic Reduction of NO by NH₃ Using a Combination of Non-Thermal Plasma and Mn-Cu/ZSM5 Catalyst. *Catalysts* **2020**, *10*, 1044. [[CrossRef](#)]
22. Zhu, B.; Zhang, L.-Y.; Li, M.; Yan, Y.; Zhang, X.-M.; Zhu, Y.-M. High-performance of plasma-catalysis hybrid system for toluene removal in air using supported Au nanocatalysts. *Chem. Eng. J.* **2020**, *381*, 122599. [[CrossRef](#)]
23. Fan, J.; Wu, H.; Liu, R.; Meng, L.; Sun, Y. Review on the treatment of organic wastewater by discharge plasma combined with oxidants and catalysts. *Environ. Sci. Pollut. Res.* **2020**. [[CrossRef](#)]
24. Mitrović, T.; Tomić, N.; Djukić-Vuković, A.; Dohčević-Mitrović, Z.; Lazović, S. Atmospheric Plasma Supported by TiO₂ Catalyst for Decolourisation of Reactive Orange 16 Dye in Water. *Waste Biomass Valorization* **2020**, *11*, 6841–6854. [[CrossRef](#)]
25. Thevenet, F.; Sivachandiran, L.; Guaitella, O.; Barakat, C.; Rousseau, A. Plasma–catalyst coupling for volatile organic compound removal and indoor air treatment: A review. *J. Phys. D Appl. Phys.* **2014**, *47*, 224011. [[CrossRef](#)]
26. Xu, S.; Bi, H.; Liu, G.; Su, B. Integration of catalytic ozonation and adsorption processes for increased efficiency of textile wastewater treatment. *Water Environ. Res.* **2019**, *91*, 650–660. [[CrossRef](#)]
27. Li, C.; Rao, Y.; Zhang, B.; Huang, K.; Cao, X.; Peng, D.; Wu, J.; Xiao, L.; Huang, Y. Extraordinary catalysis induced by titanium foil cathode plasma for degradation of water pollutant. *Chemosphere* **2019**, *214*, 341–348. [[CrossRef](#)]
28. Feng, X.; Liu, H.; He, C.; Shen, Z.; Wang, T. Synergistic effects and mechanism of a non-thermal plasma catalysis system in volatile organic compound removal: A review. *Catal. Sci. Technol.* **2018**, *8*, 936–954. [[CrossRef](#)]
29. Hinde, P.; Demidyuk, V.; Gkelios, A.; Tipton, C. Plasma Catalysis: A Review of the Interdisciplinary Challenges Faced: Realising the potential of plasma catalysis on a commercial scale. *Johns. Matthey Technol. Rev.* **2020**, *64*, 138–147. [[CrossRef](#)]
30. Voecks, G. Foam Type Catalyst System in Non-Thermal Plasma Catalytic Reactor. U.S. Patents 10/414,616, 21 October 2004.
31. Ayrault, C.; Barrault, J.; Blin-Simiand, N.; Jorand, F.; Pasquiers, S.; Rousseau, A.; Tatibouet, J. Oxidation of 2-heptanone in air by a DBD-type plasma generated within a honeycomb monolith supported Pt-based catalyst. *Catal. Today* **2004**, *89*, 75–81. [[CrossRef](#)]
32. Veerapandian, S.K.; Leys, C.; De Geyter, N.; Morent, R. Abatement of VOCs using packed bed non-thermal plasma reactors: A review. *Catalysts* **2017**, *7*, 113. [[CrossRef](#)]
33. Kogelschatz, U.; Eliasson, B.; Egli, W. Dielectric-barrier discharges. Principle and applications. *J. Phys. IV* **1997**, *7*, C4-47–C44-66. [[CrossRef](#)]
34. Zhang, K.; Zhang, G.; Liu, X.; Phan, A.N.; Luo, K. A study on CO₂ decomposition to CO and O₂ by the combination of catalysis and dielectric-barrier discharges at low temperatures and ambient pressure. *Ind. Eng. Chem. Res.* **2017**, *56*, 3204–3216. [[CrossRef](#)]
35. Zhang, H.; Ma, D.; Qiu, R.; Tang, Y.; Du, C. Non-thermal plasma technology for organic contaminated soil remediation: A review. *Chem. Eng. J.* **2017**, *313*, 157–170. [[CrossRef](#)]

36. Liu, S.; Mei, D.; Wang, L.; Tu, X. Steam reforming of toluene as biomass tar model compound in a gliding arc discharge reactor. *Chem. Eng. J.* **2017**, *307*, 793–802. [CrossRef]
37. Tu, X.; Whitehead, J.C. Plasma dry reforming of methane in an atmospheric pressure AC gliding arc discharge: Co-generation of syngas and carbon nanomaterials. *Int. J. Hydrogen Energy* **2014**, *39*, 9658–9669. [CrossRef]
38. Fridman, A.; Nester, S.; Kennedy, L.A.; Saveliev, A.; Mutaf-Yardimci, O. Gliding arc gas discharge. *Prog. Energy Combust. Sci.* **1999**, *25*, 211–231. [CrossRef]
39. Kasih, T.P.; Mangindaan, D.; Ayuputri, O.; Romulo, A.; Widyaningrum, D. Corona discharge development and its application to eliminate microorganism in raw milk. In Proceedings of the IOP Conference Series: Earth and Environmental Science, Solo, Indonesia, 13–14 November 2019; IOP Publishing: Bristol, UK, 2020; p. 012141.
40. Qu, G.; Liang, D.; Qu, D.; Huang, Y.; Liu, T.; Mao, H.; Ji, P.; Huang, D. Simultaneous removal of cadmium ions and phenol from water solution by pulsed corona discharge plasma combined with activated carbon. *Chem. Eng. J.* **2013**, *228*, 28–35. [CrossRef]
41. Talebizadeh, P.; Babaie, M.; Brown, R.; Rahimzadeh, H.; Ristovski, Z.; Arai, M. The role of non-thermal plasma technique in NO_x treatment: A review. *Renew. Sustain. Energy Rev.* **2014**, *40*, 886–901. [CrossRef]
42. Whealton, J.H.; Hansen, G.; Storey, J.; Raridon, R.; Armfield, J.; Bigelow, T.; Graves, R. Non-Thermal Plasma Exhaust Aftertreatment: A Fast Rise-Time Concept; SAE Technical Paper. 1997. Available online: <https://doi.org/10.4271/971718> (accessed on 8 December 2020).
43. Murugesan, P.; Moses, J.; Anandharamakrishnan, C. Water decontamination of using non-thermal plasma: Concepts, applications, and prospects. *J. Environ. Chem. Eng.* **2020**, *8*, 104377. [CrossRef]
44. Ould Ahmedou, S.; Rouaud, O.; Havet, M. Electrohydrodynamic enhancement of heat and mass transfer in food processes. In Proceedings of the 3rd International Symposium on Food and Agricultural Products, Naples, Italy, 24–26 September 2007.
45. Kim, H.H. Nonthermal plasma processing for air-pollution control: A historical review, current issues, and future prospects. *Plasma Process. Polym.* **2004**, *1*, 91–110. [CrossRef]
46. Van Laer, K.; Bogaerts, A. How bead size and dielectric constant affect the plasma behaviour in a packed bed plasma reactor: A modelling study. *Plasma Sources Sci. Technol.* **2017**, *26*, 085007. [CrossRef]
47. Görsmann, C. Catalytic coatings for active and passive diesel particulate filter regeneration. *Mon. Chem.* **2005**, *136*, 91–105. [CrossRef]
48. Wang, B.; Chi, C.; Xu, M.; Wang, C.; Meng, D. Plasma-catalytic removal of toluene over CeO₂-MnO_x catalysts in an atmosphere dielectric barrier discharge. *Chem. Eng. J.* **2017**, *322*, 679–692. [CrossRef]
49. Gong, S.; Sun, Y.; Zheng, K.; Jiang, G.; Li, L.; Feng, J. Degradation of levofloxacin in aqueous solution by non-thermal plasma combined with Ag₃PO₄/activated carbon fibers: Mechanism and degradation pathways. *Sep. Purif. Technol.* **2020**, *250*, 117264. [CrossRef]
50. Nguyen, D.B.; Nguyen, V.T.; Heo, I.J.; Mok, Y.S. Removal of NO_x by selective catalytic reduction coupled with plasma under temperature fluctuation condition. *J. Ind. Eng. Chem.* **2019**, *72*, 400–407. [CrossRef]
51. Hoseini, S.; Rahemi, N.; Allahyari, S.; Tasbihi, M. Application of plasma technology in the removal of volatile organic compounds (BTX) using manganese oxide nano-catalysts synthesized from spent batteries. *J. Clean. Prod.* **2019**, *232*, 1134–1147. [CrossRef]
52. Zheng, K.; Sun, Y.; Gong, S.; Jiang, G.; Zheng, X.; Yu, Z. Degradation of sulfamethoxazole in aqueous solution by dielectric barrier discharge plasma combined with Bi₂WO₆-rMoS₂ nanocomposite: Mechanism and degradation pathway. *Chemosphere* **2019**, *222*, 872–883. [CrossRef]
53. Wang, J.; Sun, Y.; Feng, J.; Xin, L.; Ma, J. Degradation of triclocarban in water by dielectric barrier discharge plasma combined with TiO₂/activated carbon fibers: Effect of operating parameters and byproducts identification. *Chem. Eng. J.* **2016**, *300*, 36–46. [CrossRef]
54. Xin, L.; Sun, Y.; Feng, J.; Wang, J.; He, D. Degradation of triclosan in aqueous solution by dielectric barrier discharge plasma combined with activated carbon fibers. *Chemosphere* **2016**, *144*, 855–863. [CrossRef]
55. Ren, Y.; Li, X.; Ji, S.; Lu, S.; Buekens, A.; Yan, J. Removal of gaseous HxCBz by gliding arc plasma in combination with a catalyst. *Chemosphere* **2014**, *117*, 730–736. [CrossRef]
56. Yuan, M.-H.; Lin, Y.-Y.; Chang, C.-Y.; Chang, C.-C.; Shie, J.-L.; Wu, C.-H. Atmospheric-Pressure Radio-Frequency Discharge for Degradation of Vinyl Chloride with Pt₂/Al₂O₃ Catalyst. *IEEE Trans. Plasma Sci.* **2011**, *39*, 1092–1098. [CrossRef]

57. Kirkpatrick, M.J.; Finney, W.C.; Locke, B.R. Plasma-catalyst interactions in the treatment of volatile organic compounds and NO_x with pulsed corona discharge and reticulated vitreous carbon Pt/Rh-coated electrodes. *Catal. Today* **2004**, *89*, 117–126. [[CrossRef](#)]
58. Jiang, N.; Hu, J.; Li, J.; Shang, K.; Lu, N.; Wu, Y. Plasma-catalytic degradation of benzene over Ag–Ce bimetallic oxide catalysts using hybrid surface/packed-bed discharge plasmas. *Appl. Catal. B Environ.* **2016**, *184*, 355–363. [[CrossRef](#)]
59. Chen, S.; Wang, H.; Shi, M.; Ye, H.; Wu, Z. Deep Oxidation of NO by a Hybrid System of Plasma–N-Type Semiconductors: High-Energy Electron-Activated “Pseudo Photocatalysis” Behavior. *Environ. Sci. Technol.* **2018**, *52*, 8568–8577. [[CrossRef](#)]
60. Jia, Z.; Amar, M.B.; Yang, D.; Brinza, O.; Kanaev, A.; Duten, X.; Vega-González, A. Plasma catalysis application of gold nanoparticles for acetaldehyde decomposition. *Chem. Eng. J.* **2018**, *347*, 913–922. [[CrossRef](#)]
61. Ray, D.; Subrahmanyam, C. CO₂ decomposition in a packed DBD plasma reactor: Influence of packing materials. *RSC Adv.* **2016**, *6*, 39492–39499. [[CrossRef](#)]
62. Roland, U.; Holzer, F.; Kopinke, F.-D. Combination of non-thermal plasma and heterogeneous catalysis for oxidation of volatile organic compounds: Part 2. Ozone decomposition and deactivation of γ -Al₂O₃. *Appl. Catal. B Environ.* **2005**, *58*, 217–226. [[CrossRef](#)]
63. Wallis, A.E.; Whitehead, J.C.; Zhang, K. Plasma-assisted catalysis for the destruction of CFC-12 in atmospheric pressure gas streams using TiO₂. *Catal. Lett.* **2007**, *113*, 29–33. [[CrossRef](#)]
64. Li, K.; Liu, G.; Gao, T.; Lu, F.; Tang, L.; Liu, S.; Ning, P. Surface modification of Fe/MCSAC catalysts with coaxial cylinder dielectric barrier discharge plasma for low-temperature catalytic hydrolysis of CS₂. *Appl. Catal. A Gen.* **2016**, *527*, 171–181. [[CrossRef](#)]
65. Tarkwa, J.-B.; Acayanka, E.; Jiang, B.; Oturan, N.; Kamgang, G.Y.; Laminsi, S.; Oturan, M.A. Highly efficient degradation of azo dye Orange G using laterite soil as catalyst under irradiation of non-thermal plasma. *Appl. Catal. B Environ.* **2019**, *246*, 211–220. [[CrossRef](#)]
66. Reddy, P.M.K.; Dayamani, A.; Mahammadunnisa, S.; Subrahmanyam, C. Mineralization of Phenol in Water by Catalytic Non-Thermal Plasma Reactor—An Eco-Friendly Approach for Wastewater Treatment. *Plasma Process. Polym.* **2013**, *10*, 1010–1017. [[CrossRef](#)]
67. Vanraes, P.; Willems, G.; Nikiforov, A.; Surmont, P.; Lynen, F.; Vandamme, J.; Van Durme, J.; Verheust, Y.P.; Van Hulle, S.W.; Dumoulin, A. Removal of atrazine in water by combination of activated carbon and dielectric barrier discharge. *J. Hazard. Mater.* **2015**, *299*, 647–655. [[CrossRef](#)]
68. Guo, H.; Jiang, N.; Wang, H.; Lu, N.; Shang, K.; Li, J.; Wu, Y. Pulsed discharge plasma assisted with graphene-WO₃ nanocomposites for synergistic degradation of antibiotic enrofloxacin in water. *Chem. Eng. J.* **2019**, *372*, 226–240. [[CrossRef](#)]
69. Ghezzer, M.; Abdelmalek, F.; Belhadj, M.; Benderdouche, N.; Addou, A. Gliding arc plasma assisted photocatalytic degradation of anthraquinonic acid green 25 in solution with TiO₂. *Appl. Catal. B Environ.* **2007**, *72*, 304–313. [[CrossRef](#)]
70. Guo, H.; Jiang, N.; Wang, H.; Shang, K.; Lu, N.; Li, J.; Wu, Y. Enhanced catalytic performance of graphene-TiO₂ nanocomposites for synergetic degradation of fluoroquinolone antibiotic in pulsed discharge plasma system. *Appl. Catal. B Environ.* **2019**, *248*, 552–566. [[CrossRef](#)]
71. Feng, J.; Zheng, Z.; Sun, Y.; Luan, J.; Wang, Z.; Wang, L.; Feng, J. Degradation of diuron in aqueous solution by dielectric barrier discharge. *J. Hazard. Mater.* **2008**, *154*, 1081–1089. [[CrossRef](#)] [[PubMed](#)]
72. Wang, T.; Qu, G.; Ren, J.; Yan, Q.; Sun, Q.; Liang, D.; Hu, S. Evaluation of the potentials of humic acid removal in water by gas phase surface discharge plasma. *Water Res.* **2016**, *89*, 28–38. [[CrossRef](#)] [[PubMed](#)]
73. Ansari, M.; Mahvi, A.H.; Salmani, M.H.; Sharifian, M.; Fallahzadeh, H.; Ehrampoush, M.H. Dielectric barrier discharge plasma combined with nano catalyst for aqueous amoxicillin removal: Performance modeling, kinetics and optimization study, energy yield, degradation pathway, and toxicity. *Sep. Purif. Technol.* **2020**, *251*, 117270. [[CrossRef](#)]
74. Jögi, I.; Erme, K.; Haljaste, A.; Laan, M. Oxidation of nitrogen oxide in hybrid plasma-catalytic reactors based on DBD and Fe₂O₃. *Eur. Phys. J. Appl. Phys.* **2013**, *61*, 24305. [[CrossRef](#)]
75. Nian, P.; Peng, L.; Feng, J.; Han, X.; Cui, B.; Lu, S.; Zhang, J.; Liu, Q.; Zhang, A. Aqueous methylparaben degradation by dielectric barrier discharge induced non-thermal plasma combined with ZnO-rGO nanosheets. *Sep. Purif. Technol.* **2019**, *211*, 832–842. [[CrossRef](#)]

76. Guo, H.; Jiang, N.; Wang, H.; Lu, N.; Shang, K.; Li, J.; Wu, Y. Degradation of antibiotic chloramphenicol in water by pulsed discharge plasma combined with TiO₂/WO₃ composites: Mechanism and degradation pathway. *J. Hazard. Mater.* **2019**, *371*, 666–676. [[CrossRef](#)]
77. Zhang, G.; Sun, Y.; Zhang, C.; Yu, Z. Decomposition of acetaminophen in water by a gas phase dielectric barrier discharge plasma combined with TiO₂-rGO nanocomposite: Mechanism and degradation pathway. *J. Hazard. Mater.* **2017**, *323*, 719–729. [[CrossRef](#)]
78. Zhang, J.; Xiong, Z.; Zhao, X. Graphene–metal–oxide composites for the degradation of dyes under visible light irradiation. *J. Mater. Chem.* **2011**, *21*, 3634–3640. [[CrossRef](#)]
79. Liu, X.; Li, W.; Hu, R.; Wei, Y.; Yun, W.; Nian, P.; Feng, J.; Zhang, A. Synergistic degradation of acid orange 7 dye by using non-thermal plasma and g-C₃N₄/TiO₂: Performance, degradation pathways and catalytic mechanism. *Chemosphere* **2020**, *249*, 126093. [[CrossRef](#)]
80. Hao, R.; Wang, G.; Jiang, C.; Tang, H.; Xu, Q. In situ hydrothermal synthesis of g-C₃N₄/TiO₂ heterojunction photocatalysts with high specific surface area for Rhodamine B degradation. *Appl. Surf. Sci.* **2017**, *411*, 400–410. [[CrossRef](#)]
81. Rahimpour, M.; Taghvaei, H.; Zafarnak, S.; Rahimpour, M.R.; Raeissi, S. Post-discharge DBD plasma treatment for degradation of organic dye in water: A comparison with different plasma operation methods. *J. Environ. Chem. Eng.* **2019**, *7*, 103220. [[CrossRef](#)]
82. Guo, H.; Wang, H.; Wu, Q.; Zhou, G.; Yi, C. Kinetic analysis of acid orange 7 degradation by pulsed discharge plasma combined with activated carbon and the synergistic mechanism exploration. *Chemosphere* **2016**, *159*, 221–227. [[CrossRef](#)] [[PubMed](#)]
83. Zhang, Y.; Xiong, X.; Han, Y.; Yuan, H.; Deng, S.; Xiao, H.; Shen, F.; Wu, X. Application of titanium dioxide-loaded activated carbon fiber in a pulsed discharge reactor for degradation of methyl orange. *Chem. Eng. J.* **2010**, *162*, 1045–1049. [[CrossRef](#)]
84. Chen, J.; Du, Y.; Shen, Z.; Lu, S.; Su, K.; Yuan, S.; Hu, Z.; Zhang, A.; Feng, J. Non-thermal plasma and BiPO₄ induced degradation of aqueous crystal violet. *Sep. Purif. Technol.* **2017**, *179*, 135–144. [[CrossRef](#)]
85. Oehmigen, K.; Hähnel, M.; Brandenburg, R.; Wilke, C.; Weltmann, K.D.; Von Woedtke, T. The role of acidification for antimicrobial activity of atmospheric pressure plasma in liquids. *Plasma Process. Polym.* **2010**, *7*, 250–257. [[CrossRef](#)]
86. Shen, Y.; Han, S.; Xu, Q.; Wang, Y.; Xu, Z.; Zhao, B.; Zhang, R. Optimizing degradation of Reactive Yellow 176 by dielectric barrier discharge plasma combined with TiO₂ nano-particles prepared using response surface methodology. *J. Taiwan Inst. Chem. Eng.* **2016**, *60*, 302–312. [[CrossRef](#)]
87. Ahmadi, E.; Shokri, B.; Mesdaghinia, A.; Nabizadeh, R.; Khani, M.R.; Yousefzadeh, S.; Salehi, M.; Yaghmaeian, K. Synergistic effect of α-Fe₂O₃-TiO₂ and Na₂S₂O₈ on the performance of a non-thermal plasma reactor as a novel catalytic oxidation process for dimethyl phthalate degradation. *Sep. Purif. Technol.* **2020**, *250*, 117185. [[CrossRef](#)]
88. Yan, X.; Yi, C.; Wang, Y.; Cao, W.; Mao, D.; Ou, Q.; Shen, P.; Wang, H. Multi-catalysis of nano-zinc oxide for bisphenol A degradation in a dielectric barrier discharge plasma system: Effect and mechanism. *Sep. Purif. Technol.* **2020**, *231*, 115897. [[CrossRef](#)]
89. Guo, H.; Jiang, N.; Li, J.; Wu, Y. Synergistic degradation of bisphenol A by pulsed discharge plasma with granular activated carbon: Effect of operating parameters, synergistic mechanism and possible degradation pathway. *Vacuum* **2018**, *156*, 402–410. [[CrossRef](#)]
90. Fan, J.; Wu, H.; Liu, R.; Meng, L.; Fang, Z.; Liu, F.; Xu, Y. Non-thermal plasma combined with zeolites to remove ammonia nitrogen from wastewater. *J. Hazard. Mater.* **2020**, *401*, 123627. [[CrossRef](#)]
91. Wang, J.; Sun, Y.; Jiang, H.; Feng, J. Removal of caffeine from water by combining dielectric barrier discharge (DBD) plasma with goethite. *J. Saudi Chem. Soc.* **2017**, *21*, 545–557. [[CrossRef](#)]
92. Sotelo, J.L.; Ovejero, G.; Rodríguez, A.; Álvarez, S.; Galán, J.; García, J. Competitive adsorption studies of caffeine and diclofenac aqueous solutions by activated carbon. *Chem. Eng. J.* **2014**, *240*, 443–453. [[CrossRef](#)]
93. Ansari, M.; Sharifian, M.; Ehrampoush, M.H.; Mahvi, A.H.; Salmani, M.H.; Fallahzadeh, H. Dielectric barrier discharge plasma with photocatalysts as a hybrid emerging technology for degradation of synthetic organic compounds in aqueous environments: A critical review. *Chemosphere* **2021**, *263*, 128065. [[CrossRef](#)]
94. Niemira, B.A. Cold Plasma Decontamination of Foods. *Annu. Rev. Food Sci. Technol.* **2012**, *3*, 125–142. [[CrossRef](#)]

95. Sang, W.; Cui, J.; Mei, L.; Zhang, Q.; Li, Y.; Li, D.; Zhang, W.; Li, Z. Degradation of liquid phase N,N-dimethylformamide by dielectric barrier discharge plasma: Mechanism and degradation pathways. *Chemosphere* **2019**, *236*, 124401. [[CrossRef](#)]

Publisher's Note: MDPI stays neutral with regard to jurisdictional claims in published maps and institutional affiliations.



© 2020 by the authors. Licensee MDPI, Basel, Switzerland. This article is an open access article distributed under the terms and conditions of the Creative Commons Attribution (CC BY) license (<http://creativecommons.org/licenses/by/4.0/>).